Microbial phenotypic heterogeneity in response to a metabolic toxin: continuous, dynamically shifting distribution of formaldehyde tolerance in *Methylobacterium extorquens* populations

Jessica A. Lee[1,5,6,7], Siavash Riazi[2,5,6], Shahla H. Nemati[3,5], Andreas E. Vasdekis[3,5,6], Benjamin J. Ridenhour[4,5], Christopher H. Remien[4,5], and Christopher J. Marx[1,5,6]

Short title

Dynamics of microbial phenotypic heterogeneity in toxin tolerance

Affiliations

[1]Department of Biological Sciences, University of Idaho, Moscow, ID

[2]Bioinformatics and Computational Biology Graduate Program, University of Idaho, Moscow, ID

[3]Department of Physics, University of Idaho, Moscow, ID

[4]Department of Mathematics, University of Idaho, Moscow, ID

[5]Center for Modeling Complex Interactions, University of Idaho, Moscow, ID

[6]Institute for Bioinformatics and Evolutionary Studies, University of Idaho, Moscow, ID

[7]current address: Global Viral, San Francisco, CA

Contributions

Jessica A. Lee*: conceptualization, formal analysis, investigation, methodology, visualization, writing—original draft preparation

Siavash Riazi*: conceptualization, formal analysis, methodology, software, visualization, writing—review and editing

Shahla H. Nemati: investigation, visualization, writing—review and editing

Andreas E. Vasdekis: funding acquisition, investigation, visualization, writing—review and editing

Benjamin J. Ridenhour: formal analysis, software, supervision, writing—review and editing

Christopher H. Remien: conceptualization, funding acquisition, formal analysis, supervision, writing—review and editing

Christopher J. Marx: conceptualization, funding acquisition, project administration, supervision, writing—review and editing

* These authors contributed equally to this work.

Corresponding authors
Jessica A. Lee: jessica.audrey.lee@gmail.com
Christopher J. Marx: cmarx@uidaho.edu

Acknowledgments
We are grateful to Jannell Bazurto, Eric Bruger, Sergey Stolyar, Nicholas Shevalier, and Joshua Wirtz for assistance in conducting *M. extorquens* experiments; to Dipti Nayak for advice and resources facilitating those experiments; to Craig Miller for advice on analyzing colony counts; to William Harcombe and Jeremy Chacón for guidance on time-lapse imaging of colony growth using flatbed scanners; to Mark Lamourine for help with software and Dan Schneider for contributions to hardware for running the scanners; and to Pål Johnsen, Alex Bradley and Jannell Bazurto for helpful comments on the manuscript. Flow cytometry was conducted at the IBEST Optical Imaging Core at the University of Idaho under the guidance of Ann Norton. Genomic DNA sample preparation and sequencing were managed by the IBEST Genomics Resources Core at the University of Idaho by Dan New, Samuel Hunter, and Matt Fagnan. IBEST is supported in part by NIH COBRE grant P30GM103324. Funding for this work came from an Army Research Office MURI sub-award to CJM (W911NF-12-1-0390), and a CMCI Pilot Grant to CJM, CHR, and AEV (parent NIH award P20GM104420).

Abstract

While microbiologists often make the simplifying assumption that genotype determines phenotype in a given environment, it is becoming increasingly apparent that phenotypic heterogeneity (in which one genotype generates multiple phenotypes simultaneously even in a uniform environment) is common in many microbial populations. The importance of phenotypic heterogeneity has been demonstrated in a number of model systems involving binary phenotypic states (e.g., growth/non-growth); however, less is known about systems involving phenotype distributions that are continuous across an environmental gradient, and how those distributions change when the environment changes. Here, we describe a novel instance of phenotypic diversity in tolerance to a metabolic toxin within wild-type populations of *Methylobacterium extorquens,* a ubiquitous phyllosphere methylotroph capable of growing on the methanol periodically released from plant leaves. The first intermediate in methanol metabolism is formaldehyde, a potent cellular toxin that is lethal in high concentrations. We have found that at moderate concentrations, formaldehyde tolerance in *M. extorquens* is heterogeneous, with individual cells' minimum tolerance levels ranging between 0 mM and 8 mM. This form of heterogeneity is continuous in terms of threshold (in the range of maximum tolerances possible), yet binary in outcome (at a given formaldehyde concentration, cells either grow normally or die, with no intermediate phenotype), and it is not associated with any detectable genetic mutations. Moreover, tolerance distributions within the population are dynamic, changing over time in response to growth conditions. We characterized this phenomenon using bulk liquid culture experiments, colony growth tracking, flow cytometry, time-lapse microscopy, and genome resequencing. Finally, we used mathematical modeling to better understand the processes by which cells change phenotype, and found evidence for both stochastic, bidirectional phenotype diversification and responsive, directed phenotype shifts, depending on the growth substrate and the presence of toxin.

Introduction

Microbes are individuals. Even in seemingly simple unicellular organisms, phenotype is not always the straightforward product of genotype and environment; cells with identical genotypes in identical environments may nonetheless demonstrate cell-to-cell diversity in the expression of any of a number of traits. Frequently overlooked in everyday microbiology experiments, the phenomenon of cell-to-cell phenotypic heterogeneity has drawn increasing attention in recent decades both from a systems biology perspective and from an evolutionary perspective, as well as for its consequences to applied fields such as medicine (e.g., antibiotic persistence [1]; cancer cell drug tolerance [2,3]) and biological engineering [4].

Some forms of population heterogeneity might be considered trivial: molecular interactions within cells are inherently noisy. All genes might be expected to be expressed at slightly different levels among different cells [5–7], and historical contingency (e.g., pole age, asymmetrical division of macromolecules) can also create inherent diversity within microbial populations, independent of signals from the environment [8–10]. Naturally, evolution imposes some pressure on organisms to limit the noise in pathways that are essential for life; what is more remarkable is that some pathways seem to be selected for increased noise, and in many cases that noise is further amplified by feedback circuits, enabling a population to split into discretely different phenotypes. Specifically, genes involved in stress response and in metabolism have been found to show higher heterogeneity in expression than those in other pathways [11], and many of the well-understood examples of binary phenotypes involve stress response (antibiotic persistence [12]; sporulation [13]), or carbon transport and use (lactose utilization in *E. coli* [14]; diauxic switch in *S. cerevisiae* [15,16]). While some forms of phenotypic noise may have little fitness impact, phenotypic heterogeneity involving binary phenotypes is argued in many cases to offer an evolutionary advantage, as a strategy to facilitate diversifying bet-hedging or division of labor [11,17]. In many cases, the genetic basis of phenotypic differentiation is known, and laboratory evolution studies have demonstrated how populations can evolve the timing or

117 frequency of that differentiation in response to environmental selection [18,19].
118 Moreover, it is argued that phenotypic heterogeneity influences the rate of genotypic
119 evolution either by creating an "epigenetic load" that contributes to extinction [20], or by
120 allowing populations to adapt faster to changing environments and by increasing the
121 opportunities for mutations to arise and reach fixation [21,22].
122
123 Besides cases of binary phenotypes or modest phenotypic noise around a population
124 mean, a third possibility involves phenotypes that fall along a continuous gradient.
125 Fewer such phenomena have been described [11], but some examples include
126 populations in which cells have a range of levels of stress tolerance: for instance, a
127 genetically chloramphenicol (Cm)-resistant *E. coli* strain exhibits a wide, continuously-
128 varying distribution of maximum concentrations of Cm that individual cells can tolerate.
129 The population splits into growing and non-growing subpopulations in the presence of
130 Cm, and the proportion of growing cells varies according to the environmental Cm
131 concentration [23]. This effect is mediated by a positive-feedback interaction between
132 intracellular chloramphenicol acetyltransferase (CAT) activity and innate cell growth;
133 thus the ultimate fate of an individual cell depends on its initial internal CAT activity,
134 which can vary continuously among cells. If such a population were to experience shifts
135 in environmental Cm concentrations, the population distribution of per-cell CAT activity
136 levels could presumably shift as a consequence of either cellular responses (e.g., CAT
137 upregulation), or simply by selection against sensitive cells; however, this has not been
138 described. Analogous population-level phenotype distribution shifts have been explored
139 only through mathematical modeling, for instance in the case of human cancer cells
140 exhibiting a gradient of tolerances to cytotoxic drugs [24]. In this case, it is assumed that
141 random epimutations result in small phenotypic variations in drug tolerance, and that
142 drug exposure leads to selection upon that diversity. However, experimental work would
143 be necessary to verify whether modeling accurately predicts cell population dynamics,
144 or whether other processes—such as those in which cells sense drug concentrations
145 and respond with phenotype shifts—might also play a role. Examples of phenotypic
146 heterogeneity such as these two cases, in which a population with a continuous
147 phenotype distribution interacts dynamically with the environment to undergo dramatic

shifts in population distributions, pose complex—yet unanswered—questions about the importance of phenotypic heterogeneity to population-level fitness in diverse environments.

Here we present a novel example of a continuously-distributed phenotype in an environmentally relevant microorganism, *Methylobacterium extorquens*, and describe the dynamics of that phenotype distribution in response to shifts in its growth environment. *M. extorquens*, a species of *Alphaproteobacteria* found ubiquitously on plant leaves, is a methylotroph: it can grow on reduced single-carbon compounds such as methanol, which is emitted from leaves through the activity of plant pectin methylesterases [25]. The first intermediate in methanol metabolism is the potent toxin formaldehyde [26,27], an electrophile that can cause cellular damage through its reactions with macromolecules, and is lethal to microorganisms [28]. In *M. extorquens*, formaldehyde is produced in the periplasm through the oxidation of methanol by methanol dehydrogenase (MDH); in the cytoplasm it is then oxidized via a tetrahydromethanopterin (H_4MPT)-dependent pathway. *M. extorquens* therefore exists in a tension between the two goals of rapid substrate utilization and prevention of the accumulation of a toxic intermediate. The importance of formaldehyde oxidation for single-carbon metabolism has been demonstrated by the inability of H_4MPT-pathway mutants to grow in the presence of methanol when they possess a functional MDH [29]. However, although MDH activity is constitutive, it has also been observed that downstream single-carbon assimilation pathways are up-regulated only in the presence of methanol; the consequence is that when cells previously grown on a multicarbon substrate are first exposed to methanol, formaldehyde production initially outpaces consumption so drastically that it is excreted into the medium [26]. This is just one example of many potential situations in which cellular formaldehyde accumulation poses a threat to *M. extorquens*, and yet we know very little about how the species copes with formaldehyde toxicity.

As an initial step toward understanding the effect of formaldehyde toxicity on *M. extorquens*, we conducted time-kill experiments in which we exposed cells to a range of

179 formaldehyde concentrations in batch liquid culture and monitored their viability over
180 time. To our knowledge, previous research on formaldehyde toxicity in *M. extorquens*
181 has consisted only of single-timepoint shock experiments, or a pulse of methanol added
182 to succinate-grown cultures to cause cellular formaldehyde production [29]. We hoped
183 that making time-resolved measurements in extreme formaldehyde conditions would
184 shed light on both large-scale patterns of toxicity and on cell behavior near the minimum
185 bactericidal concentration (MBC). Indeed, quite unexpectedly, we found cell-to-cell
186 variation in the MBC within isogenic populations of *M. extorquens*. We confirmed this to
187 be a phenomenon of phenotypic diversity at the single-cell level, and investigated its
188 dynamic population-level consequences, using a combination of liquid culture
189 experiments, colony growth tracking, flow cytometry, time-lapse microscopy, genome
190 resequencing, and mathematical modeling.
191
192
193 **Results**
194
195 ***Formaldehyde-induced death occurs at an exponential, concentration-dependent***
196 ***rate at 5 mM and above***
197 In order to better understand the physiological effects of the toxic metabolite
198 formaldehyde on *M. extorquens*, we initially conducted a series of experiments in which
199 we added formaldehyde to methanol growth medium and assessed the relationship
200 between toxin concentration and mortality in well-mixed liquid batch culture. We found
201 that concentrations ≥5 mM elicited loss of viability (as measured in colony-forming units,
202 CFUs) at an exponential rate, and the rate of death increased with increasing
203 formaldehyde concentration (Fig. 1). A concentration of 15 mM was sufficient to
204 eliminate all detectable viable cells within 1.5 hours (approximately half of one
205 generation time). These time-kill curves indicate that formaldehyde-induced death can
206 be modeled as a single-hit process [30], as is often observed for other multi-target lethal
207 agents such as radiation and heat [31], and some bactericidal antibiotics [32,33]. Given
208 that the precise mechanism of formaldehyde-induced mortality remains unknown but
209 likely involves multiple cellular targets, it is noteworthy that formaldehyde-induced death

210 over time did not seem to involve substantial "shoulders" or "tails" as is sometimes
211 observed with other agents [33], and that we observed no saturation of death rate at the
212 concentrations tested. In analogy to bactericidal antibiotics, our results suggested that
213 the minimum bactericidal concentration (MBC) of formaldehyde for *M. extorquens* is 5
214 mM.
215
216 ***During exposure to moderate formaldehyde concentrations, population trajectory***
217 ***abruptly shifts from decreasing to increasing over time***
218 Follow-up experiments on longer timescales (3–4 days) revealed that assessing MBC
219 was in fact not straightforward: lower concentrations had an effect on *M. extorquens*
220 growth as well. Exposure to formaldehyde concentrations between 3 and 5 mM allowed
221 normal growth of *M. extorquens* as measured by optical density (OD_{600}), but only after
222 an apparent lag time of several hours to days. Higher formaldehyde concentrations
223 induced longer lags, but growth subsequently resumed, and formaldehyde
224 concentration had no effect on growth rate (for 0, 3, 4, and 5 mM respectively, specific
225 growth rate (r) was 0.212±0.038, 0.208±0.045, 0.238±0.002, and 0.230±0.018 h^{-1},
226 where ± indicates 95% confidence interval; p=0.237 for the effect of treatment group on
227 growth rate by ANOVA) (Fig. S1). To better understand the apparent lag in these
228 conditions, we measured cell viability over time during formaldehyde exposure
229 experiments. CFU measurements revealed that the apparent "lag time" was in fact not a
230 lag, but rather a period of exponentially decreasing cell counts followed by an abrupt
231 transition to increasing counts (Fig. 2, round gray symbols and line). These dynamics
232 repeated themselves across multiple biological replicates at multiple formaldehyde
233 concentrations, with remarkable consistency in the timing of the transition between
234 population decrease and increase. At a concentration of 4 mM formaldehyde, this
235 transition occurred at approximately 20 hours. Upon recovery, the increase in CFUs
236 was exponential and indistinguishable from growth rates on methanol in the absence of
237 external formaldehyde (r=0.215±0.001 for 0 mM; r=0.202±0.030 for 4 mM; p=0.063 by
238 Welch's t-test) (Fig. 2).
239

240 We explored several hypotheses to explain the abrupt decrease-then-increase transition
241 we observed during formaldehyde exposure. These included: 1) consumption of
242 formaldehyde by the cells; 2) the existence of formaldehyde-resistant genetic mutants;
243 3) phenotypic changes in the plating efficiency of cells due to formaldehyde-induced
244 damage and its repair; 4) the existence of a subpopulation of phenotypically (but not
245 genetically) formaldehyde-tolerant cells.
246
247 ***Population recovery occurs while formaldehyde concentrations in the medium***
248 ***remain high***
249 One explanation for the abrupt change from population decline to population increase
250 might be a change in environmental conditions: for instance, cooperative behavior to
251 metabolize a toxin to sublethal levels can result in population rescue even if not all cells
252 are tolerant, as has been observed with antibiotics [34]. We therefore investigated the
253 possibility that formaldehyde consumption had reduced the toxin concentration in the
254 medium: in formaldehyde exposure experiments with 4 mM formaldehyde, we
255 monitored formaldehyde concentrations in the medium for 80 hours, a period that
256 encompassed the death and regrowth phases. Although *M. extorquens* is capable of
257 metabolizing formaldehyde, we found that a measurable decrease in the concentration
258 of the toxin only occurred at the very end of the growth period in batch culture, more
259 than 40 hours after the decrease-then-increase transition (Fig. 2, black symbols and
260 line). A change in the toxicity of the environment was therefore not responsible for the
261 change in population trajectory.
262
263 ***Genetic mutations are not responsible for population recovery***
264 The next most parsimonious explanation was that the observed growth was due to a
265 small pre-existing subpopulation of formaldehyde-tolerant mutants whose existence
266 became apparent only after the death of the sensitive majority. To assess this
267 possibility, we grew cells in the presence of 4 mM formaldehyde for 80 hours as
268 described above, then subcultured them into fresh medium without formaldehyde for 6
269 generations (using succinate as the growth substrate), followed by another subculture
270 into formaldehyde-containing medium. The population decrease-then-increase

271 dynamics were recapitulated, indicating that formaldehyde tolerance was not
272 transmitted in a manner consistent with genetic heritability and that the descendants of
273 cells tolerant to 4 mM formaldehyde were re-sensitized in its absence (see "Transitions
274 between tolerance phenotypes," below, for more detail).
275
276 In addition, we prepared genomic DNA from cells that had grown in the presence of
277 formaldehyde (the 80-hour timepoint of a 4 mM formaldehyde exposure experiment),
278 and used this for whole-genome resequencing. The resequenced genome was
279 compared to the published genome sequence of wild-type *M. extorquens* PA1 and to
280 that of an *M. extorquens* population grown without formaldehyde; no evidence was
281 found for SNPs, deletions, insertions, or gene duplications in the formaldehyde-selected
282 population. These sequencing data, along with the instability of the formaldehyde
283 tolerance phenotype, indicate that the heterogeneous formaldehyde tolerance we have
284 observed in *M. extorquens* is not due to genetic mutations.
285
286 ***Population recovery is not due to changes in plating efficiency***
287 Having ruled out both environmental change and genetic mutations as explanations for
288 the sharp transition between population decrease and increase during formaldehyde
289 exposure, we pursued the possibility that the observed dynamics might be due to a
290 change in phenotype. As our evidence for population dynamics thus far was based on
291 counts of colony-forming units on agar medium, one possibility was that the phenotypic
292 change might be related to the ability of cells to form colonies. In this scenario,
293 formaldehyde exposure might cause cellular damage resulting in a decrease in cells'
294 ability to form colonies and their entry into a viable-but-not-culturable (VBNC) state [35],
295 and the inflection point at 20 hours represented the beginning of recovery of these same
296 cells, rather than turnover of the population.
297
298 To investigate whether there had been population turnover, we carried out a cell
299 proliferation assay, which enabled us to interrogate single-cell growth dynamics in liquid
300 culture without plating (as in [36]). We used a nontoxic fluorescent membrane linker dye
301 to stain the population prior to conducting a 4 mM formaldehyde exposure experiment

302 as described above, and then assessed the trajectory of per-cell fluorescence over time
303 by flow cytometry. In exponentially growing populations, the membrane dye of each
304 parent cell was divided between its two daughter cells, and per-cell fluorescence
305 decreased uniformly across the population as the number of cells increased (Fig. 3,
306 upper left). In non-growing populations, as when *M. extorquens* was exposed to 20 mM
307 formaldehyde, membrane dye remained in the cells and did not fade, and per-cell
308 fluorescence remained the same (Fig. 3, lower left). However, in an *M. extorquens*
309 population treated with 4 mM formaldehyde, two populations were evident: one group of
310 cells that retained the same membrane fluorescence throughout the experiment, and
311 another group of cells that increased in number and decreased in per-cell membrane
312 fluorescence, indicating normal growth in the presence of formaldehyde (Fig. 3, right).
313 At 4 mM, the growing population was observable only after ~37 hours of incubation,
314 consistent with a population that began in extremely low abundance relative to the non-
315 growing population. These data indicate that there was population turnover, and that the
316 increase in viable cell counts was in fact due to the growth of a tolerant, rare
317 subpopulation of cells that remained active in the presence of formaldehyde.
318
319 ***Phenotypically tolerant subpopulation is present prior to formaldehyde exposure***
320 Given our evidence against genetic mutants, a fourth hypothesis was that the observed
321 growth was due to a small subpopulation of cells that were phenotypically (but not
322 genetically) highly tolerant to formaldehyde. Stress-tolerant individuals may arise in
323 microbial populations stochastically, or they may do so in response to an environmental
324 signal [37]. To investigate whether the hypothesized formaldehyde-tolerant cells were
325 present in the original population or were induced during the course of formaldehyde
326 exposure, we monitored the abundance of formaldehyde-tolerant CFU over time.
327 Specifically, we repeated the 4 mM formaldehyde exposure experiment and plated the
328 cells harvested at each timepoint on selective agar culture medium (4 mM
329 formaldehyde, allowing the growth of only tolerant cells) and permissive medium
330 (without formaldehyde, to enumerate all cells). We found that at the beginning of the
331 experiment, the *M. extorquens* population already contained a detectable subpopulation
332 of cells that were able to form colonies in the presence of 4 mM formaldehyde. This

333 subpopulation comprised only a small portion of the total number of cells (a frequency of
334 ~10^{-4} in the total population of ~$2x10^6$ cells) (Fig. 2, orange diamond symbols and lines).
335 And while the total abundance of cells decreased at an exponential rate between 0 and
336 20 hours, the formaldehyde-tolerant subpopulation increased at a constant rate for
337 nearly the entire course of the experiment, such that after 20 hours the population was
338 dominated by cells tolerant to 4 mM formaldehyde.
339
340 ***Formaldehyde-tolerant subpopulation shows no evidence of formaldehyde-***
341 ***induced cell damage***
342 The fact that the tolerant subpopulation increased at a rate commensurate with
343 standard growth in formaldehyde-free media suggests that these tolerant cells may
344 have escaped formaldehyde-induced mortality and any damage that might impede or
345 delay growth. However, some stress-tolerant phenotypes, such as persister cells, are
346 characterized by slow growth or even absence of growth [12]. We therefore looked
347 more closely at the growth phenotypes of the tolerant subpopulation: specifically,
348 whether they differed in their rate of colony growth, or in the time required to initiate a
349 colony, relative to normal unstressed cells. We repeated the 4 mM formaldehyde
350 exposure experiment described above, this time using time-lapse imaging to monitor the
351 growth of colonies resulting from timepoint samples plated on both selective and
352 permissive plates. Plates were incubated on a flatbed photo scanner and images
353 captured hourly and processed to extract per-colony statistics (Fig. S2), in a manner
354 similar to previous studies investigating cell damage and dormancy at the single-cell
355 level [38–40].
356
357 We found that within the total population, which consisted of sensitive cells at a
358 frequency of 10^{-5} at the beginning of the experiment, formaldehyde exposure prior to
359 plating did indeed induce a lag in colony formation, such that each hour of formaldehyde
360 exposure led to an increase in colony arisal time (the time necessary to form a
361 detectable colony) of approximately 4.80 hours (r^2=0.766 by linear regression, p<0.005)
362 (Fig. 4). This pattern held true for the first 16 hours of exposure, until most of the
363 sensitive cells lost viability entirely. At 16 hours, we observed a clear bimodality on the

364 permissive plates, with approximately half of the cells arising late and the other half
365 arising early, and the abundance of the early arisers on the permissive plates was
366 consistent with the abundance of the tolerant subpopulation (all colonies on the
367 selective plates). However, on the selective plates, we observed no relationship
368 between arisal time and the length of formaldehyde exposure prior to plating
369 (slope=-0.091 hours lag per hour exposure, r^2=0.0639, p<0.005), supporting the
370 hypothesis that the tolerant subpopulation is in a different physiological state that does
371 not experience formaldehyde damage in the same way as the sensitive subpopulation.
372 Furthermore, we observed no trend in average growth rate due to formaldehyde
373 exposure time (slope=-2.83x10^{-4} hours lag per hour exposure, r^2=6.62x10^{-4}, p=0.123),
374 although colonies from samples that had been exposed for longer had more varied
375 growth rates (there was a positive linear relationship between exposure time and the log
376 of the median average deviation of growth rate, p<0.05 for both permissive and
377 selective plates).
378
379 ***Tolerant subpopulation behavior is observable at the single-cell level***
380 As a final step in confirming single-cell phenotypic heterogeneity in formaldehyde
381 tolerance, we observed growth of single cells directly using high-resolution time-lapse
382 phase-contrast microscopy of cultures embedded in agar pads. This method allowed us
383 to observe the division times and potential morphological aberrations of individual cells
384 and their progeny in microcolonies over the first 12 hours of growth. Because the cells
385 tolerant to 4 mM formaldehyde are only present at a frequency of approximately 10^{-4} in
386 the initial population, we conducted formaldehyde exposure at a lower concentration,
387 2.5 mM formaldehyde, at which plating experiments (see below) suggested that ~1-4%
388 of cells would be able to grow. Indeed, we found that 11 out of 546 cells (1.97%) were
389 able to grow at that formaldehyde concentration, compared to 100% of the 256 cells
390 observed in the no-formaldehyde condition (Fig. 5). In addition, all the cells that grew in
391 the presence of formaldehyde did so normally: we found no significant effect of
392 formaldehyde on cell division time (median doubling time at 0 mM: 2.58 hours; at 2.5
393 mM: 2.58 hours; p=0.262 by Mann-Whitney U-test). We did observe that cells in
394 formaldehyde took slightly longer to complete the first division (median lag time was

395 1.25 hours later in formaldehyde; $p<0.001$, Mann-Whitney U); this may indicate minor
396 cell damage or a very modest inhibitory effect of formaldehyde in the medium, or it may
397 have resulted from slight differences in the preparation of the cells (as it was technically
398 infeasible to conduct the two experiments simultaneously). Of the variance in doubling
399 times among individual cells, most was explained by the microcolony to which the cell
400 belonged ($p=0.001$, PERMANOVA) but not by formaldehyde treatment ($p=0.323$),
401 indicating that there is some heritability in growth rates (Fig. 5). Finally, we did not
402 witness any partial-growth or impaired-growth phenotypes: the 535 cells that were
403 unable to grow in the presence of formaldehyde showed no detectable elongation or
404 other change in morphology.
405
406 ***Formaldehyde-tolerant cells grow at normal rates on methanol but marginally***
407 ***slower on succinate***
408 Our single-cell observations of growth suggested that formaldehyde-tolerant cells grow
409 normally; the formaldehyde tolerance phenotype thus differs from other microbial stress-
410 tolerance phenotypes previously described (e.g., sporulation, persistence) in that it does
411 not require cells to sacrifice proliferative ability by entering a non-growing state in order
412 to survive stressful conditions. Moreover, our observations of colony arisal times
413 suggested that tolerant cells avoid the damage incurred by formaldehyde-sensitive
414 cells. We therefore investigated the possibility that other fitness tradeoffs might exist, by
415 comparing non-selected *M. extorquens* cells with those of a tolerant population (i.e.,
416 selected by growth in liquid culture at 4 mM formaldehyde).
417
418 We observed no difference in the resistance of the tolerant population to several other
419 chemical stressors (hydrogen peroxide, and the antimicrobial compounds rifampicin,
420 vancomycin, cefoxitin, novobiocin, nalidixic acid, ciprofloxacin, erythromycin,
421 kanamycin, gentamicin, chloramphenicol, colistin) during growth on agar medium (data
422 not shown). However, we did observe differences in growth rate when comparing the
423 tolerant and naive (non-selected) populations side-by-side in liquid batch culture,
424 depending on whether the growth substrate was methanol (15 mM) or the non-
425 methylotrophic substrate succinate (3.5 mM). In methanol medium, the two populations

426 grew at similar rates (naive: r=0.222±0.023; tolerant: r=0.202±0.051 h^{-1}); however, on
427 succinate medium, the naive population grew faster (naive: r=0.270±0.002 h^{-1}; tolerant:
428 r=0.215±0.030 h^{-1}) (Fig. S3). The differences in growth rate among the four treatments
429 were in this case not found to exhibit statistically significant differences by ANOVA
430 (F=2.617, p=0.123 for the model; p=0.940 for the planned contrast between the two
431 populations on methanol and p=0.136 on succinate). However, the apparent slight
432 advantage of the naive population over the tolerant on succinate was attributable to the
433 fact that the naive population grew faster on methanol than on succinate, consistent
434 with observations commonly made in our lab (Fig. S7) and reported in the literature [27].
435 If the formaldehyde-tolerant population does not show the typical increased growth rate
436 on succinate, it would indicate that tolerance is associated with methylotrophic
437 metabolism, and may provide a clue as to the conditions in which tolerant cells could be
438 out-competed by sensitive cells in the environment.
439
440 ***Phenotypic heterogeneity in formaldehyde tolerance is a continuous phenotype***
441 As described previously, many cases of phenotypic heterogeneity display binary
442 phenotypes (e.g., persistent or not [12]). On the other hand, a few display a continuous
443 distribution (e.g., resistance to chloramphenicol along a gradient of possible MBC levels
444 [23]). While formaldehyde exposure results in a binary outcome for each cell—either
445 growth, or cessation and death—we sought to quantify the ratio of these outcomes
446 along a gradient of formaldehyde concentrations, by plating *M. extorquens* onto agar
447 medium containing formaldehyde at concentrations between 1 and 10 mM in
448 increments of 1 mM. The results showed no evidence of a bimodal distribution along the
449 concentration axis; rather, tolerance is continuous, peaks at 0 mM, and declines
450 exponentially and predictably with increasing formaldehyde concentration (Fig. 6). We
451 were able to detect cells with tolerance levels as high as 6 mM. While we found growth
452 stage to have an effect on the abundance of tolerant cells (populations in exponential
453 growth were shifted toward slightly higher tolerance), the qualitative shape of the
454 distribution remained the same. Furthermore, populations that were cultured in the
455 same way and sampled at the same growth stage reproduced similar formaldehyde
456 tolerance distributions across multiple days (Fig. S4). Notably, all colonies that grew on

457 formaldehyde agar medium were of uniform shape and size, suggesting that tolerant
458 cells shared similar arisal times and growth rates, as was previously observed at 4 mM
459 (Fig. 4). In addition, cell proliferation assays with the membrane-intercalating dye
460 performed at concentrations of 2, 3, and 5 mM formaldehyde qualitatively recapitulated
461 the previously described population turnover seen with the assay at 4 mM, and
462 supported the relationship between concentration and abundance of tolerant cells (Fig.
463 S5). Thus, although the consequence of formaldehyde upon an individual cell is binary
464 (growth or not, rather than a range of growth rates), the distribution of tolerance (i.e.,
465 MBC values) within a population is continuous.
466
467 ***Transitions in tolerance phenotypes over time depend on growth conditions***
468 Given our previous observations that growth conditions can change the shape of the
469 formaldehyde tolerance distribution in a population, and that formaldehyde tolerance,
470 once selected for, can be lost, we sought to characterize more precisely the processes
471 by which tolerance distributions might shift in a population. Specifically, we hoped to
472 better understand the relative importance of formaldehyde-mediated selection (whereby
473 formaldehyde exposure kills sensitive cells) and active changes made by cells to alter
474 phenotype. We began by monitoring the abundance of each subpopulation, at tolerance
475 levels between 0 and 10 mM in 1 mM intervals, over time during a 4 mM formaldehyde
476 exposure experiment. We monitored for 20 hours, the time it takes for most sensitive
477 subpopulations to lose viability entirely (Fig. 2). As expected, we found that in these
478 conditions, all subpopulations tolerant to <4 mM decrease in abundance and the
479 subpopulations tolerant to ≥4 mM increase, resulting after 20 hours in a tolerance
480 distribution with a maximum at 4 mM (Fig. 7, S6).
481
482 In order to measure the rate at which phenotypic tolerance in the population returns to
483 its original distribution, we conducted a formaldehyde-free regrowth experiment.
484 Specifically, we transferred the selected, high-tolerance population to liquid medium
485 without formaldehyde and monitored the changes in tolerance distributions for the next
486 24 hours in two different conditions: one with methanol as the sole carbon substrate,
487 and the other with succinate. We observed a marked difference between the two growth

488 conditions in their effect on population tolerance distributions over time. In the succinate
489 medium, only the populations with low tolerance increased in abundance, whereas
490 those with high tolerance *decreased* in abundance, so the shape of the distribution
491 shifted back toward that of naive *M. extorquens* cells (Fig. 7, S6). The observation that
492 tolerant cells decreased in abundance even during an increase in the overall population
493 suggests that cells were shifting in phenotype from high tolerance to low. In contrast, in
494 the methanol medium, all tolerant subpopulations increased in abundance at the same
495 rate: the overall shape of the distribution, with its high proportion of tolerant cells, stayed
496 the same. Growth in methanol medium thus maintains phenotypic formaldehyde
497 tolerance in a population that is *already* tolerant, even though it does not induce or
498 select for tolerance in sensitive populations. This unexpected substrate-based
499 hysteresis (historical dependence) may be due to the small amount of formaldehyde
500 produced inside the cell during methylotrophic metabolism, which might trigger cells,
501 either through a stress-response mechanism or through regulation of methylotrophic
502 metabolism, to remain in a tolerant phenotype even if external formaldehyde is not
503 present in the growth medium.
504
505 ***Mathematical modeling elucidates cellular phenotype transition processes***
506 ***underlying population-level shifts***
507 To better understand what biological processes might be responsible for the
508 observations of the three experiments described above, we developed a mathematical
509 model to test several hypotheses. We examined the dependence of death rate upon
510 formaldehyde concentration in the medium and tolerance phenotype of the cell. We also
511 asked whether shifts in the tolerance distribution could be explained by growth and
512 selective death alone, or involved other processes. To this end, we tested the effect of
513 introducing two processes by which cells might actively transition along the 1-
514 dimensional axis of "phenotype space": one involving random phenotype transitions in
515 any direction (a Brownian motion, or diffusion, process), and one involving directed
516 transitions toward either higher or lower tolerance (an advection process) (Fig. 8). We
517 evaluated models based on their ability to reproduce the dynamics from the three
518 experimental conditions shown in Figure 7: selection during a 4 mM formaldehyde

exposure experiment, and formaldehyde-free regrowth of the selected high-tolerance population on either succinate or methanol.

We modeled the dynamics of *M. extorquens* populations during exposure to formaldehyde with a partial differential equation:

$$\partial_t N(x,t) = r_c N(x,t) - H(x,F)N(x,t) + D\,\partial_{xx}N(x,t) + v\,\partial_x N(x,t) \qquad (1)$$

The population is structured by phenotype, with $N(x,t)$ denoting the concentration of cells (CFU*mL^{-1}) with formaldehyde tolerance x (mM) at time t (hours). The formaldehyde tolerance of a cell is defined as the maximum concentration of formaldehyde in which the cell can grow. The model tracks cells in a well-mixed, closed population as they grow on substrate c at per capita rate r_c (h^{-1}), die at per capita rate $H(x,F)$, and change phenotype (Fig. 8). We assume that phenotypic transitions occur due to two processes, diffusion with coefficient D (mM^2*h^{-1}) and advection with rate v (mM*h^{-1}) (where mM refers to tolerance level). The death function $H(x,F)$ describes per capita death rate of cells as a function of formaldehyde concentration and is given by:

$$H(x,F) = \alpha(F - bx) \text{ if } x < F \qquad (2)$$

where F (mM) is the formaldehyde concentration, α (mM^{-1}*h^{-1}, where mM refers to formaldehyde in the medium) is the death rate, and b (mM tolerance / mM formaldehyde) specifies the sensitivity of the death rate to a cell's formaldehyde tolerance level.

For each of the three experimental conditions separately, we used maximum likelihood to fit the parameters α, b, D, and v to the data, and used a likelihood ratio test on the nested models to determine the best model structure. For the selection scenario, we began with a 1-parameter model with $\alpha > 0$ and the other parameters equal to 0, and tested 2-, 3-, and 4-parameter models sequentially, at each step choosing the model with the highest likelihood as long as it was significantly better than the simpler model (results in Table 1). For regrowth (where there is no death), we fit only v and D. In each

550 of the three experimental conditions, our model was able to reproduce the experimental
551 observations extremely well (pseudo-R^2 = 0.973, 0.993, 0.991 for the formaldehyde
552 selection, methanol regrowth, and succinate regrowth conditions respectively) (Table 1).
553
554 ***Phenotype transition processes change according to growth conditions***
555 We examined not only what the best-fit value was for each of the four parameters of
556 interest, but also whether there was support (by likelihood ratio test) for including each
557 of the parameters. The three experimental conditions differed from one another in both
558 considerations, suggesting that the rate and nature of phenotype transition processes
559 change depending on environment.
560
561 In the formaldehyde selection regime, the best model included both death parameters
562 (α=0.202±0.022 h^{-1}, b=0.770±0.147), but for the phenotype transition parameters, only
563 diffusion (D=0.019±0.006 mM^2*h^{-1}) and not advection. This indicates that the changes
564 we observed in the formaldehyde tolerance distribution during formaldehyde exposure
565 are due not only to death, but also involve phenotype shifts consistent with diffusion.
566 Diffusion leads to the spread of phenotypes consistent with what was observed in the
567 model after 20 hours, including the presence of population density at x=2 and x=3 mM
568 (which otherwise would have decreased to below detection in the absence of transitions
569 from higher-tolerance phenotypes) and some cells at x>6 (which were not observed in
570 the initial population, but may have resulted from transitions from lower-tolerance
571 phenotypes) (Fig. 9).
572
573 For the scenarios involving regrowth of a selected population on formaldehyde-free
574 medium, the parameter estimates were markedly different from those in the selection
575 condition, and from each other. For methanol growth, we found support only for very
576 mild advection toward lower tolerance (v=0.018±0.006 $mM*h^{-1}$). For succinate growth,
577 we found support for both advection (v=0.285±0.026 $mM*h^{-1}$) and diffusion
578 (D=0.033±0.010 mM^{2*} h^{-1}); the advection term for succinate was an order of magnitude
579 greater than that for methanol, indicating strong shifts in the direction of lower tolerance
580 when high-tolerance cells are grown on succinate. This agrees with our earlier

qualitative observations that growth on succinate, but not on methanol, leads *M. extorquens* populations to lose formaldehyde tolerance rapidly and in general to undergo diversifying phenotype transitions. Furthermore, it supports our hypothesis that formaldehyde tolerance is associated with methylotrophic growth, and implies that further work is needed not only to understand the mechanism of phenotypic formaldehyde tolerance shifts in *M. extorquens* but also the regulation of those processes.

The inclusion of b in the model specifically allowed us to test the possibility that a cell's formaldehyde tolerance might determine not only the threshold concentration above which it dies, but also the rate at which it dies (Fig S8). That is, if $b=0$, the death rate is equivalent for all cells regardless of tolerance level as long as tolerance is below the threshold; but for $0<b\leq1$, cells with lower tolerance levels die more quickly than those with higher tolerance, and the strength of this dependence upon x scales with the value of b. The value of b that best fit our data was 0.770 (Table 1), indicating that formaldehyde-tolerant cells may receive some protection from the tolerance phenotype even at concentrations above their MBC. However, both the experimental results and the model simulation showed a bimodal phenotype distribution after formaldehyde exposure, consistent with a weak dependence of death rate from tolerance level (Fig. S8). Future experiments with a greater number of observations at low-tolerance phenotypes would better elucidate the relationship between tolerance and death dynamics.

Discussion

We have described here a novel example of phenotypic tolerance to a metabolic toxin that is continuously distributed across individual cells in a clonal microbial population, where the phenotypic heterogeneity is present even when all cells inhabit the same environment, but its distribution undergoes dynamic shifts when the population experiences different environmental conditions. Wild-type populations of genetically

612 identical *Methylobacterium extorquens* cells grown in well-mixed liquid medium contain
613 individuals with maximum formaldehyde tolerance levels ranging from 0 mM to 6 mM
614 (and tolerance at up to 8 mM has been observed after selection); although the
615 distribution is continuous and exponentially decreasing, individuals show binary
616 growth/non-growth phenotypes at any given formaldehyde concentration, and may
617 transition among phenotypic states through both bidirectional phenotype diversification
618 and responsive, directed phenotype shifts.
619
620 When might *M. extorquens* experience formaldehyde in its natural environment, and at
621 what concentrations? *M. extorquens* excretes formaldehyde during the first stages of
622 the switch between multi-carbon and single-carbon metabolism [26]; in addition,
623 formaldehyde is a metabolic intermediate in the consumption of many lignin-derived
624 aromatic compounds [41,42], and we have observed lignin degraders to excrete
625 formaldehyde into the growth medium at millimolar levels during growth in batch liquid
626 culture on methoxylated aromatic compounds (Lee & Marx, unpublished). Thus, it is
627 possible that, in the environment, formaldehyde concentrations in the millimolar range
628 might accumulate transiently on the microscale, especially within cell aggregates such
629 as those observed on plant leaves [43]. However, it is also possible that formaldehyde
630 tolerance is an outward manifestation of a cellular state that has quite a different
631 relevance in the native environment of *M. extorquens*: high tolerance to local (external)
632 formaldehyde may indicate a high capacity for tolerating (internal) formaldehyde
633 generated through methylotrophic metabolism. As such, this phenomenon may provide
634 insight into processes that are general to many organisms whose central metabolic
635 pathways involve toxic intermediates [44,45].
636
637 The mechanisms by which high-tolerance cells can maintain normal growth in the
638 presence of seemingly lethal concentrations of formaldehyde, and by which that ability
639 is transmitted to progeny, remain yet to be discovered. Phenotypic formaldehyde
640 tolerance could involve a specific stress-response system. Alternatively, it may involve
641 components of methylotrophic metabolism, as suggested by the association between
642 maintenance of formaldehyde tolerance and methanol growth, and the potentially lower

643 fitness of tolerant cells during succinate growth. Previous reports have found phenotypic
644 heterogeneity in the related strain *M. extorquens* AM1 in growth rate, cell size, gene
645 expression levels, and ability to switch between carbon substrates [8,46,47]; those
646 forms of diversity may have a similar basis to the phenomenon discussed here.
647 Because of the crucial role that the H_4MPT pathway of formaldehyde oxidation plays in
648 removing cellular formaldehyde and thus allowing methylotrophic growth [29], very small
649 variations in the activity of H_4MPT pathway enzymes might have a significant impact on
650 a cell's capacity to tolerate externally-provided formaldehyde. Assuming that
651 formaldehyde transport into the cytoplasm is diffusion-driven (as no means of active
652 transport has yet been discovered), phenotypic diversity in formaldehyde oxidation
653 capacity would result in a range of internal concentrations across cells. Furthermore, if
654 cells that begin to experience formaldehyde-mediated damage to proteins and other
655 macromolecules begin to lose their capacity to oxidize formaldehyde, this would
656 generate a positive feedback circuit that could ultimately determine a binary outcome to
657 whether a cell lives or dies. The fact that we observed no elongation at all from the cells
658 that could not grow at 2.5 mM suggests that this postulated positive feedback
659 mechanism acts on a very fast timescale (i.e., minutes, not hours). This mechanism
660 could explain both the continuous relationship between concentration and abundance of
661 tolerant cells, and the binary nature of the "live normally or die immediately" distribution
662 observed at each specific formaldehyde level, similar to the topology of interactions
663 observed in the case of chloramphenicol resistance described earlier [23].
664
665 Viewed this way, formaldehyde tolerance exhibits potential parallels with other
666 examples in which phenotype switching is mediated by a bistable switch: for instance,
667 pyrimidine-mediated colony type switching in *Bacillus subtilis* [48], chloramphenicol
668 resistance [23], and lactose utilization *E. coli* [49]. In all these cases, the balance
669 between the concentrations of multiple intracellular components determines the
670 phenotype of a cell, with cells pushed away from the threshold into one of two states by
671 a positive feedback loop, and often maintained there by hysteresis (as we observed in
672 the maintenance of formaldehyde tolerance among cells growing on methanol, Fig. 7).
673 Making changes that alter the ratios of the components, through control of either gene

674 expression or of the environment, alters the frequency of cells near the threshold and
675 thereby the ratio of cells in each of the two bistable states (as we observed when
676 altering formaldehyde concentrations in the medium). Furthermore, these systems are
677 analogous to threshold traits observed in animals, in which observed discontinuous
678 phenotypes (e.g., two phenotypic morphs) arise from a continuously distributed
679 underlying trait [50]. The threshold model of quantitative genetics describes a constant
680 threshold that determines which values of the underlying trait generate each of the
681 phenotypic morphs; evolutionary and environmental changes can lead to shifts in the
682 underlying trait distributions that result in different ratios of the two morphs being
683 observed in different environments. As we have shown here, the continuously
684 distributed trait of *M. extorquens* formaldehyde tolerance similarly changes with
685 environment; however, in this case the threshold (environmental formaldehyde
686 concentration, which separates tolerant cells from sensitive) is external and may also be
687 manipulated. *M. extorquens* therefore provides a convenient model system in which to
688 probe the dynamics of threshold traits.
689
690 Both stress response proteins and metabolic enzymes are inherited during cell division,
691 so either pathway provides a hypothesis for the heritability of formaldehyde tolerance
692 that we observed after formaldehyde was removed. Lineage dependence has been
693 observed in numerous cases of phenotypic heterogeneity, and is often cited as
694 evidence that the phenotype of interest is dictated by a heritable component of the cell
695 with a moderately long lifetime (e.g., pole age [8], stress-protective protein aggregates
696 [51]). In these cases, the random transitions in phenotype that we modeled as diffusion
697 can be explained by asymmetric partitioning of cell contents [52], whereas the directed
698 transitions that we modeled as advection could be due to responsive up- or down-
699 regulation of the production/degradation or (in)activation of the molecules involved.
700
701 The balance between stochastic and responsive phenotype differentiation processes,
702 as mechanisms for increasing population fitness in unpredictable environments, has
703 often been discussed as a question of the relative costs and benefits of each. Both
704 mathematical modeling [53,54] and laboratory evolution [18,55] have demonstrated that

705 either mechanism—or both simultaneously—can be selected for, with evolutionary
706 outcomes dictated by the cost of sensing, the timing of environmental change, the
707 reliability of environmental cues, and the spatial structure of the community. The fact
708 that we observed non-directed general diversification in our populations in some growth
709 conditions, and environment-responsive, directed phenotype shifts in others, strongly
710 suggests that that differentiation in formaldehyde tolerance in *M. extorquens* is not due
711 simply to unavoidable molecular noise, but rather it is a regulated process conferring a
712 fitness advantage.
713
714 If it exists, the nature of such a fitness advantage remains unclear; it is tempting to ask
715 why *M. extorquens* does not maintain a population composed solely of high-tolerance
716 cells. The evolutionary basis for phenotypic heterogeneity in genetically identical
717 populations of microorganisms is frequently ascribed to diversifying bet-hedging, in
718 which a species in an unpredictably changing environment constitutively generates
719 progeny with multiple phenotypes to ensure that at least a few will thrive in any
720 circumstances [11,56]. The surface of the plant leaf, the native environment of *M.*
721 *extorquens*, is indeed unpredictable: cells depend for growth upon a combination of
722 gaseous methanol excreted from plant stomata [57] and other metabolites such as
723 simple organic acids produced by the plant or by other microorganisms [58]. The
724 emission of methanol, dependent on the metabolic state of the plant host and the
725 conductivity of the stomata, undergoes large temporal variation [59]. It is therefore
726 plausible that this environment could select for heterogeneity in formaldehyde toxicity
727 response and in growth on non-methylotrophic substrates. An alternative evolutionary
728 explanation is division of labor, which is an advantageous strategy when a particular
729 activity is beneficial to the population but incurs some cost to the individual carrying it
730 out [54]. In our experiments, the tolerant subpopulation is capable of detoxifying
731 formaldehyde from the growth medium; although in batch culture this occurs too late to
732 prevent the sensitive cells from dying (Fig. 2), this might occur differently in a spatially-
733 structured community such as cell aggregates on the surface of a plant leaf.
734

735 Importantly, both bet-hedging and division of labor assume fitness tradeoffs among the
736 phenotypes being diversified. Although tolerant cells may be slower than sensitive cells
737 at growth on a multicarbon substrate (Fig. S8), it is unclear whether this disadvantage is
738 substantial enough to explain the low frequency of high-tolerance cells in our *M.*
739 *extorquens* populations. Further mathematical modeling could be used to quantify the
740 effects of these growth tradeoffs and to explore conditions that could lead to the
741 evolution of the steady-state distribution that we have observed in the lab. Furthermore,
742 while phenotypic heterogeneity has been studied in great depth both in laboratory
743 populations and in populations simulated by mathematical modeling, there remains a
744 dearth of research on organisms in the natural environments in which they evolved
745 [56,60]. Future experiments examining the dynamics of phenotypic formaldehyde
746 tolerance among *M. extorquens* cells growing on plant leaves, and among related
747 methylotrophs in other environmental niches, will be essential to establishing the
748 environmental relevance of this phenomenon.
749
750
751 **Materials and Methods**
752
753 ***Bacterial strains and culture conditions***
754 All experiments were conducted with *M. extorquens* PA1 CM2730, an otherwise wild-
755 type strain that contains a deletion of the cellulose synthesis operon to prevent cell
756 clumping [61]. All cultures were grown at 30 °C in MPIPES mineral medium (30 mM
757 PIPES, 1.45 mM K_2HPO_4, 1.88 mM NaH_2PO_4, 0.5 mM $MgCl_2$, 5.0 mM $(NH_4)_2SO_4$, 0.02
758 mM $CaCl_2$, 45.3 μM $Na_3C_6H_5O_7$, 1.2 μM $ZnSO_4$, 1.02 μM $MnCl_2$, 17.8 μM $FeSO_4$, 2 μM
759 $(NH_4)_6Mo_7O_{24}$, 1 μM $CuSO_4$, 2 μM $CoCl_2$, 0.338 μM Na_2WO_4, pH 6.7) [61], either in
760 liquid form or with the addition of 15 g/L Bacto-Agar (BD Diagnostics) for solid medium.
761 Growth substrates consisted either of methanol provided at 15 mM (in liquid medium) or
762 125 mM (in solid medium); or succinate provided at lower concentrations to ensure the
763 same molarity of carbon as in methanol conditions: 3.5 mM succinate (in liquid) or 15
764 mM (in solid). Unless otherwise noted, all liquid cultures were grown as a 20 mL volume
765 in 50 mL-capacity conical flasks, capped with Suba-Seal rubber septa (Sigma-Aldrich)

766 to prevent the escape of volatile compounds, with shaking at 250 rpm. Extensive testing
767 in our lab has shown that cultures grown thus are not limited by oxygen availability and
768 grow at the same rate as in flasks with loose lids. Prior to the beginning of each
769 experiment, cultures were streaked from freezer stock onto solid medium and allowed to
770 grow for 4 days to form colonies, and for each biological replicate a single colony was
771 used to inoculate 5 mL of liquid medium in a culture tube and allowed to grow 24 hours.
772 This overnight culture, containing ~$2x10^8$ CFU/mL at stationary phase, was used as the
773 inoculum for the growth experiment.
774
775 ***Formaldehyde exposure experiments***
776 Growth and tolerance distribution dynamics in the presence of low concentrations of
777 formaldehyde were assessed by inoculating stationary-phase culture at a 1:64 dilution
778 (for an initial population of ~$3x10^6$ CFU/mL) into fresh MPIPES + methanol medium
779 containing formaldehyde at the specified concentration (4 mM unless otherwise stated).
780 Cultures were grown under the conditions described above (20 mL MPIPES, Suba-Seal
781 septa, shaking at 30 °C) and sampled periodically to measure cell viability and
782 formaldehyde concentration. Sampling was conducted as follows: 100 µL of culture was
783 removed through the septum using a sterile syringe and transferred to a trUVue low-
784 volume cuvette (Bio-Rad) to read optical density at 600 nm using a SmartSpec Plus
785 spectrophotometer (Bio-Rad). An additional 200 µL of culture was removed and
786 transferred to a microcentrifuge tube. The culture was centrifuged for 1 minute at 14,000
787 x g; the supernatant was removed and saved for formaldehyde measurement (see
788 below) and the cell pellet was resuspended in 200 µL fresh MPIPES medium without
789 carbon substrate or formaldehyde. Cells were then subjected to serial 1:10 dilutions in
790 MPIPES to a final dilution of 10^{-6}. From each of the seven dilutions, three replicates of
791 10 µL were pipetted onto culture plate containing MPIPES-methanol solid medium to
792 form spots (total: 21 spots per sample per plate type). In experiments measuring
793 formaldehyde tolerance distribution, multiple plate types were used, each type
794 containing a different concentration of formaldehyde (see "Formaldehyde tolerance
795 distributions," below). The spots were allowed to dry briefly in a laminar flow hood, then
796 lids were replaced and plates were stored in plastic bags and incubated at 30 °C for 4

797 days before colonies were counted. For each replicate set of seven spots, the two
798 highest-dilution spots with countable colonies were enumerated and summed, then
799 multiplied by 1.1 times the lower of the two dilution factors to calculate the original
800 number of colony-forming units (CFU) in the sample. For each sample, the mean and
801 standard deviation of the three replicate spot series was calculated.
802
803 For the measurement of death rates in the presence of high concentrations of
804 formaldehyde, cells were grown in MPIPES medium with methanol and no
805 formaldehyde until they reached an OD_{600} of 0.1 (~ $1x10^8$ CFU/mL, mid-exponential
806 phase), then formaldehyde was added to the desired final concentration and
807 immediately mixed well. Growth conditions were as described above and samples were
808 taken every 20 minutes to measure formaldehyde concentrations and cell viability.
809 Growth rates were measured by fitting a linear relationship between time and the binary
810 logarithm of CFU/mL using the lm function; differences among growth rates were
811 assessed using either the anova function or the t.test function, in the stats package.
812
813 Fresh 1 M formaldehyde stock was made weekly by combining 0.3 g paraformaldehyde
814 powder (Sigma Aldrich), 9.95 mL ultrapure water, and 50 µL 10 N NaOH solution in a
815 sealed tube, and immersing in a boiling water bath for 20 minutes to depolymerize.
816 Formaldehyde was measured using the method of Nash [62]. In brief, equal volumes of
817 sample (or standard) and Nash Reagent B (2 M ammonium acetate, 50 mM glacial
818 acetic acid, 20 mM acetylacetone) were combined in a microcentrifuge tube and
819 incubated for 6 minutes at 60 ºC. Absorbance was read on a spectrophotometer at 412
820 nm. For experiments involving large numbers of samples, the same assay was
821 conducted in a 96-well polystyrene flat-bottom culture plate (Olympus Plastics): 100 µL
822 each of sample and Reagent B were combined in each well of a culture plate and the
823 plate was incubated at 60 ºC for 10 minutes before reading absorbance at 432 nm on a
824 Wallac 1420 Victor2 multilabel plate reader (Perkin Elmer). A clean plate was used for
825 each assay; each plate contained each sample in triplicate as well as a standard curve
826 run in triplicate.
827

828 ***Genome resequencing of formaldehyde-tolerant subpopulation***
829 Whole-genome sequencing was conducted on an *M. extorquens* population selected for
830 high formaldehyde tolerance, to determine whether there were any genetic changes
831 associated with the formaldehyde tolerance phenotype. In addition, the genomes of two
832 non-selected *M. extorquens* populations were prepared, sequenced, and analyzed at
833 the same time using the same methods, as controls to enable us to distinguish
834 mutations specific to formaldehyde tolerance from any that may have accrued in our
835 laboratory strain since the sequencing of the published genome.
836
837 Tolerant cells were selected via a 4 mM formaldehyde exposure experiment as
838 described above, and allowed to grow until stationary phase; the tolerance distribution
839 of each population was assayed to confirm that cells were indeed 100% tolerant to 4
840 mM formaldehyde (see "Formaldehyde tolerance distributions," below). From each of 3
841 replicate populations, 2 mL of culture (~2.2×10^8 CFU/sample) were harvested. Genomic
842 DNA was extracted using the Epicentre Masterpure Complete DNA and RNA
843 Purification Kit (Epicentre/Illumina), following the manufacturer protocol for DNA
844 purification, and the three populations were pooled. Library preparation was carried out
845 by the IBEST Genomic Resources Center at the University of Idaho (Moscow, ID):
846 genomic DNA was used to make shotgun libraries using the TruSeq PCR-free Library
847 Prep Kit (Illumina) with the HiSeq-length insert option (short), amplified using KAPA
848 (Illumina), cleaned using magnetic beads (MagBio), and quantified using fluorometry
849 prior to pooling. The pooled library was quality-checked by Fragment Analyzer
850 (Advanced Analytical) and quantified with the KAPA Library Quantification Kit for ABI
851 Prism (Kapa Biosystems). Sequencing was conducted in a 1x100 run on a HiSeq 4000
852 at the University of Oregon Genomics and Cell Characterization Core Facility (Eugene,
853 OR); reads were demultiplexed by the facility using bcl2fastq Conversion Software
854 (Illumina).
855
856 Genomic data was analyzed for evidence of mutations using breseq 0.32.1 [63] with
857 default settings, using the published genome of *M. extorquens* PA1 (NC_010172 [64])
858 as a reference, and comparing with a similar dataset from an *M. extorquens* CM2730

859 population that had been grown without formaldehyde. No predicted mutations were
860 found in the formaldehyde-tolerant population that were not also found in the non-
861 formaldehyde population. Three genomic loci (MEXT_RS13110, MEXT_RS12285/
862 MEXT_RS12290 intergenic region, MEXT_RS02695) carried SNPs identified as
863 "marginal mutation predictions" at a frequency of <33%, but further analysis revealed
864 these to be due to assembly errors in extremely repeat-rich regions that appear in both
865 the tolerant and control samples. Areas containing marginal mutation predictions were
866 further checked by PCR amplification and Sanger sequencing of the original DNA.
867 Primers used were 5'- CTCTCCGCCGAAGTGGT-3' and 5'-
868 GCCTTCCTCGGGTTCAAGGG-3' (for MEXT_RS02695); 5'-
869 CAGGGAACGCTCGTAGAGG-3' and 5'- CCACCGTGAAACGCACCGTA-3' (for
870 MEXT_RS12285-RS12290); and 5'-GTAGACCGCCTCCGAGACTT-3' and 5'-
871 GTAGACCGCCTCCGAGACTT-3' (for MEXT_RS13110). Genome resequencing data
872 have been deposited in the NCBI SRA database under BioProject PRJNA504295.
873
874 ***Cell proliferation assay***
875 Growth versus non-growth phenotypes in bulk liquid culture were assessed using a cell
876 proliferation assay with the non-toxic green fluorescent membrane linker dye PKH67
877 (Sigma-Aldrich). To ensure that *Methylobacterium* cells could be easily distinguished
878 from background events in flow cytometry, experiments were conducted using *M.*
879 *extorquens* CM3839, a strain identical to CM2730 but constitutively expressing the red
880 fluorescent protein mCherry at the *hpt* locus [65]. Stationary-phase cultures were
881 stained and washed following the manufacturer protocol for PKH67, modified only in
882 that all centrifugation steps were carried out for 1 minute at 14,000 x g. OD_{600} was
883 measured after staining to account for any loss of cells, and inoculation density was
884 adjusted to ensure an initial population of ~$3x10^6$ CFU/mL. Stained cells were used in a
885 formaldehyde exposure experiment as described above, with treatments at 0, 1, 2, 3, 4,
886 5, and 20 mM formaldehyde. Unstained cells were grown alongside the stained cells as
887 a control to assess whether staining affected growth rate or viability; no measurable
888 difference in growth was detected. Samples were taken periodically by syringe and
889 washed of formaldehyde as described above; instead of plating for viability, they were

890 resuspended in 1 M (3%) formaldehyde as a fixative and stored at 4 °C until analysis by
891 flow cytometry. Immediately prior to analysis, cells were centrifuged once more and
892 resuspended in fresh medium to remove excess formaldehyde.
893
894 Flow cytometry was conducted in the IBEST Imaging Core at the University of Idaho
895 using a CytoFLEX S benchtop flow cytometer (Beckman Coulter); each sample was
896 analyzed at a flow rate of 10 µL/min for 3 minutes to ensure that an equal volume was
897 examined from each. Output was gated to allow only events with a mCherry signal
898 (ECD-area channel, excitation: 488 nm, emission: 610/620 bp) $>10^3$. Per-cell membrane
899 fluorescence was measured in the FITC-area channel (excitation: 488 nm; emission:
900 525/40 bp). Data analysis was conducted in R v.3.4.3 [66] using the flowCore package
901 [67] to interpret fcs files and the ggplot2 package [68] to generate plots.
902
903 ***Formaldehyde tolerance distributions***
904 The distribution of formaldehyde tolerance phenotypes within a population was
905 assessed by plating cell cultures onto agar plates containing formaldehyde. MPIPES
906 medium was prepared with agar, autoclaved, and cooled to 50 ºC; then methanol and
907 formaldehyde to the desired final concentration were rapidly mixed in, and the agar was
908 poured into 100 mm petri dishes. The dish lids were immediately replaced and plates
909 were cooled on the benchtop. Plates were stored at 4 ºC and used within 1 week of
910 pouring. CFU were plated and enumerated as described above. This method has a limit
911 of detection of 1.65×10^{-7} (an abundance of 34 CFU/mL is necessary to observe 1 cell
912 per 30 µL plated, and the total cell population tested was 2×10^8 CFU/mL; therefore the
913 least-abundant subpopulation that could be detected, disregarding the effects of
914 Poisson distributions at lower λ, is one with an average frequency of 1.65×10^{-7} within
915 the total population).
916
917 To assess whether formaldehyde concentrations in agar culture plates changed over
918 time due to volatilization, plates containing 0, 2, 4, 6, 8, and 10 mM of formaldehyde
919 were assayed for formaldehyde content before and after a 3-day incubation, stored
920 together in the same bag, at 30 ºC. A small amount of agar (~0.1 g) was excised from

921 the plate, melted, diluted 1:10 in MPIPES medium, and assayed using the Nash
922 protocol (described above). Each plate was assayed in triplicate. No change in
923 concentration was detected in any of the plates (Fig. S9).
924
925 ***Colony arisal time and growth rates***
926 To measure the effect of formaldehyde damage on colony time and growth rates, colony
927 growth was monitored using Epson Perfection V600 flatbed photo scanners.
928 Formaldehyde exposure experiments were carried out on *M. extorquens* as described
929 above, but diluted samples were spread-plated rather than spotted onto culture plates:
930 100 µL of one dilution was spread on each plate. Lids were lined with sterile black felt to
931 reduce condensation and increase contrast, and plates were placed agar-side-down on
932 scanner beds. Each culture contained precisely 30 mL of agar medium, to ensure
933 uniformity of nutrient supply and hydration status across all plates; temperature probes
934 were included between plates on scanner beds to monitor temperatures for consistency.
935 Scanners were placed in a 30 °C incubator and image acquisition was controlled by a
936 computer running Linux Mint, using a cron job for scheduling and a custom bash script
937 employing the utility scanimage to take images once per hour.
938
939 Images were processed using a custom Python 3.5.6 script employing scikit-image
940 v.0.12.1 [69] to identify colonies and measure their areas in pixels. Subsequent data
941 analysis was conducted in R: double colonies and non-colony objects were removed
942 from the dataset, colony arisal time was measured as the first timepoint at which colony
943 area measured greater than 100 pixels, and colony growth rate was measured by fitting
944 a linear relationship between time and the binary logarithm of colony area using the lm
945 function. Variability among growth rates was assessed as the median average deviation
946 (MAD) within the colonies from a single timepoint, using the mad function in the stats
947 package. The effect of formaldehyde exposure time on colony arisal time, colony growth
948 rate, and MAD was calculated using simple linear models using the lm function. Further
949 details of both image analysis and colony growth statistics are included in Supplemental
950 Materials (Fig. S2).
951

952 ***Time-lapse microscopy***

953 To analyze the formaldehyde-dependent heterogeneous response in lag-phase and
954 elongation rates of *M. extorquens*, we employed single-cell time-lapse microscopy using
955 a phase-contrast inverted microscope (Leica, DMi8) equipped with an automated stage.
956 For image acquisition, we employed a 60x (PH2, NA: 0.7) magnification objective and a
957 sCMOS camera (Hamamatsu, ORCA-Flash 4). Time-lapse imaging was performed
958 under ambient conditions (regulated at 26 ºC ± 1 ºC) with a 5-minute period using
959 automated routines (Molecular Devices, Methamorph). All reported experiments were
960 performed once.

961

962 For imaging with single-cell resolution, 2 µL of 10x diluted stationary-phase cells
963 (approximately $6x10^5$ CFU) grown in liquid MPIPES-methanol without formaldehyde
964 were introduced on 1 mm thick agar pads pre-deposited on a glass coverslip. The
965 culture solution was allowed to dry for approximately 10 minutes within a biosafety
966 cabinet and was subsequently covered with a second coverslip. Individual bacteria were
967 therefore immobilized at the agar-coverslip interface, allowing them to grow in two
968 dimensions. Specific locations (200x150 μm^2) were monitored in parallel, selected by
969 evaluating the distance between individual cells at the beginning of each experiment so
970 that expanding micro-colonies would not overlap spatially at later time points. On
971 average, 40 microcolonies per location were imaged, with approximately 8-10 individual
972 cells per microcolony in the final timepoint. ImageJ [70] and manual curation were
973 employed for cell segmentation and tracking (Fig. S10).

974

975 To prepare the pads, MPIPES-agar medium was prepared as described above
976 ("Bacterial strains and culture conditions"), and melted at 70 ºC for approximately 2
977 hours using a convection oven. Subsequently, methanol was introduced to the agar
978 medium to a final concentration of 125 mM. Specific to the formaldehyde tolerance
979 experiments, formaldehyde was also added to a final concentration of 2.5 mM. In all
980 experiments, a polydimethylsiloxane (PDMS, Sylgard 184, Dow Corning) frame was
981 employed to cover all free edges of the agar pads. This step was employed to minimize
982 formaldehyde evaporation during time-lapse imaging. To fabricate these membranes,

983 PDMS monomer was mixed with its catalyst at a 10:1 ratio, degassed, and cured at 70
984 ºC for approximately 2 hours. Subsequently, the cured PDMS was cut to an area of
985 25×50 mm^2, including a 21×47 mm^2 internal aperture, where the melted agar was
986 subsequently introduced.
987
988 Analysis of cell doubling times and microcolony lag times was conducted in R. The
989 wilcox.test function was used to compare the formaldehyde-treated population with the
990 control population by Mann-Whitney Wilcoxon test [71]. The relative effects of
991 formaldehyde treatment and colony lineage were assessed by permutational
992 multivariate ANOVA using distance matrices (PERMANOVA) [72], with the adonis
993 function in the vegan package [73].
994
995 For all microscopy experiments, an aliquot of the same culture used for the microscopy
996 experiment was simultaneously grown in batch liquid culture with same concentration of
997 formaldehyde, and CFUs in both the total and formaldehyde-tolerant populations were
998 tracked over time, as a control. In all cases, the growth of the liquid culture proceeded
999 as expected and the frequency of formaldehyde-tolerant cells matched that observed in
1000 the microscopy experiment.
1001
1002 ***Assays on selected formaldehyde-tolerant subpopulations: fitness trade-offs***
1003 ***formaldehyde-free regrowth experiments***
1004 For characterization of the formaldehyde-tolerant subpopulation, a 4 mM formaldehyde
1005 exposure experiment was conducted as described above to select for cells with a
1006 minimum tolerance level of 4 mM. Once cultures had reached stationary phase
1007 (approximately 80 hours), they were used within 4 hours for further experiments.
1008
1009 Assessment of tolerance to antimicrobial drugs and to hydrogen peroxide were carried
1010 out using a disk susceptibility test: liquid exponential-phase cultures grown on methanol
1011 in standard conditions were diluted to an OD_{600} of 0.3, then spread using a sterile swab
1012 onto the surface of MPIPES-methanol-agar plates and allowed to dry. A BBL Sensi-Disc
1013 (Becton-Dickinson), impregnated with one antibiotic compound at a set concentration,

1014 was then placed on top of the plate. Plates were incubated at 30 °C for 48 hours to
1015 allow a lawn to grow; the diameter of the clearing zone around the antibiotic disk was
1016 then measured and compared between the naive and selected high-tolerance
1017 populations.
1018
1019 To compare growth rates on different carbon substrates, three selected subpopulations,
1020 and three naive populations not previously exposed to formaldehyde, were diluted 1:64
1021 into fresh MPIPES medium containing either methanol or succinate, and each of those
1022 was transferred into the wells of a 48-well tissue culture plate (Corning Costar) with 640
1023 µL culture in each of three replicate wells. Plates were incubated on a Liconic LPX44
1024 incubator shaker at 650 rpm, and OD_{600} was read using a Wallac 1420 Victor2 plate
1025 reader. Growth rates were calculated in R using timepoints during the period of
1026 exponential growth (between 5-18 hours for methanol growth and 5-22 hours for
1027 succinate), by fitting a linear relationship between time and the binary logarithm of the
1028 OD using the lm function in R. Rates were calculated for each well individually; for each
1029 biological replicate, the mean and standard deviation of the three replicate wells was
1030 calculated. Statistical tests of differences among growth rates consisted of analysis of
1031 variance using the anova function from the stats package, and planned contrasts
1032 calculated using the lsmeans and contrast functions from the lsmeans package.
1033
1034 To assess tolerance distribution dynamics during formaldehyde-free regrowth, three
1035 selected subpopulations were each diluted 1:64 into two batches of fresh MPIPES liquid
1036 medium, one batch containing methanol and the other succinate. Dilutions were grown
1037 in standard flask conditions as described above, but with loose caps instead of Suba
1038 Seals. Cultures were sampled every 4 hours for serial dilution and plating as described
1039 above, with each sample plated onto each of 7 plates containing different levels of
1040 formaldehyde (0, 2, 4, 6, 8, 10, or 12 mM). Plates were incubated and colonies were
1041 counted as described above.
1042

1043 ***Mathematical model***

1044 Growth, death, and phenotype transitions of *M. extorquens* populations were modeled
1045 using a partial differential equation (PDE; Equation 1). The full code for parameter fitting
1046 and model selection is included as an R notebook in the Supporting Information, File
1047 S1. Over the time periods for which we ran the model simulation, there was no effective
1048 change in the concentration of either of the growth substrates (methanol, succinate;
1049 each of which have extremely low half-saturation constants [74,75]) or formaldehyde
1050 (Fig. 2); these compounds were therefore not explicitly included as time-dependent
1051 variables in the model. Furthermore, given that tolerance either has no effect upon
1052 growth on methanol, or a mild effect upon succinate growth, we use a single value of r_c
1053 for all values of x.

1054

1055 Modeling was conducted in R. The PDE was solved numerically by vectorized ODEs,
1056 where each ODE corresponded to a discrete bin within tolerance space of 0.01 mM
1057 formaldehyde. A finite difference grid was created using the setup.grid.1D function, and
1058 advection and diffusion were calculated using the advection.1D or tran.1D function as
1059 appropriate for the different models, in the ReacTran package v. 1.4.3.1 [76]. The
1060 vectorized ODEs were solved using the ode.1D function from the package deSolve
1061 v1.21 [77], with the lsoda method [78]. Zero-flux boundary conditions for Equation 1 are
1062 given by: $\partial_x N(0,t)=0$ and $\partial_x N(L,t)=0$. The lower boundary was set as x=0 because
1063 tolerance cannot fall below 0. The upper boundary ($x=L$) for each growth condition was
1064 set higher than the highest experimentally observed value, sufficiently large so as not to
1065 constrain the upward transition of cells in phenotypic space.

1066

1067 *Initial conditions*

1068 The experimentally measured distributions of formaldehyde tolerances in the original
1069 populations were used as initial conditions in all model runs. Because we found that
1070 populations exhibit a slight shift toward higher average tolerance within 2 hours of
1071 transitioning from the stationary (non-growing) to the exponential (growing) phase (Fig.
1072 6), and because our model specifically focuses on growth phenomena and does not
1073 capture behavior in stationary phase, we chose the 2-hour tolerance distribution as our

initial condition (Fig. S7) in order to avoid artefacts that would result from using the 0-hour stationary-phase distribution. Three biological replicates were generated and the average of the three used to generate the distribution.

Because the model is continuous, whereas the experimental data were obtained at a resolution of 1.0 or 2.0 mM formaldehyde in tolerance space, the initial conditions for the model were generated by fitting a monotone cubic spline using the function splinefun in R with method "hyman," to interpolate cell abundances for values of *x* at intervals of 0.01 mM (Fig. S7). Subsequently, for comparison of model results with experimental results, the model results were summed in 1 mM or 2 mM intervals to re-obtain coarse bins matching the resolution of the experimental data (as in Fig. 9).

In the model, *x* denotes tolerance as the *maximum* tolerance level of a cell or subpopulation. However, our experimental CFU counts are cumulative in that regard (*i.e.*, the cells that form colonies on culture plates containing 3 mM formaldehyde include those with a maximum tolerance of not just 3 mM but also 4 mM, 5 mM, and 6 mM). For the purposes of carrying out the model, we therefore transformed the empirical tolerance distributions in the experimental datasets to calculate the actual (non-cumulative) number of CFU at each phenotype level using the following formula:

$$N(x) = \widehat{N}(x) - \widehat{N}(x+h) \qquad (3)$$

where $N(x)$ is the number of cells that uniquely have a given tolerance level x, $\widehat{N}(x)$ is the number of cells measured experimentally as CFU on culture plates with formaldehyde concentration x, and h is the step size between categories in data (1 mM for Fig. 7a; 2 mM for Figs. 7b-c). This transformation to the non-cumulative distribution was used after spline fitting to calculate the initial distributions for the model, and model results are shown in this format in Fig. 9a-b and Fig. S8b. However, for all other purposes, including parameter fitting as well as display in Figs. 9c-d and S11, model results were transformed back to the cumulative distribution for comparison with the experimental results. Both forms of the data are displayed in the R notebook (File S1).

1105

1106 A further adjustment to data from all timepoints was made to account for the
1107 experimental limit of detection (34 CFU/mL) in measuring formaldehyde tolerance
1108 distributions: growth of originally undetected low-frequency cells in the high-tolerance
1109 phenotypes could potentially be mistaken as transition into those phenotypes from
1110 lower-tolerance phenotypes. To assess whether such undetected cells would make a
1111 difference to the model results, we generated a set of "extended" CFU counts in which
1112 we made the extreme correction of adding 1 CFU to the experimental observations (the
1113 equivalent of 90.9 CFU/mL for that replicate, or 30.3 CFU/mL if averaged across the
1114 three replicates) at high formaldehyde concentrations where the observation had been 0
1115 CFU. This correction was made to the data from all timepoints, according to the
1116 following rules:
1117 1. If 0 colonies were observed in all technical replicates, add 1 colony to one of the
1118 replicates.
1119 2. Only do (1) if either:
1120 a) there is an observation of ≥1 colony at a higher concentration than the one being
1121 considered, OR
1122 b) it is the first concentration beyond the last observation of ≥1 colony.
1123

1124 We carried out parameter fitting and model selection for the 4 mM formaldehyde
1125 selection experiment using both the original dataset and the extended one (as
1126 described in the previous paragraph). Although the use of the extended dataset resulted
1127 in minor differences in the estimated parameters (Tables 1 and S1, Fig. S11), the same
1128 form of the model was favored (the 3-parameter model with α, d, and b), and the
1129 pseudo-R^2 (0.973) was slightly better than for the version using the original dataset
1130 (0.970). We interpreted this to mean that the inclusion or omission of rare undetected
1131 cells at high tolerance levels makes little difference to any biologically relevant
1132 conclusions, but that our correction may allow for a better model fit. We therefore
1133 proceeded with only the extended dataset for the models describing formaldehyde-free
1134 regrowth, and all parameter and statistical values given in the text are those for the
1135 extended data.

1136

1137 *Parameter estimation*

1138 Growth rates (r_c for substrate c, either methanol or succinate, h^{-1}) and their standard
1139 errors were estimated from fitting experimental data of growth of a wild-type, naive
1140 population on either succinate or methanol as a primary carbon source, in the absence
1141 of formaldehyde (Fig. S7). Linear regression was used to fit the relationship between
1142 cell count and time for the exponential portion of three replicate growth curves, using
1143 the lm function in R. The growth rate on methanol was 0.195±0.001 h^{-1} and the growth
1144 rate on succinate was 0.267±0.005 h^{-1}, where ± denotes 95% confidence interval.

1145

1146 The death rate (α), dependence of death on tolerance (b), diffusion (D), and advection
1147 (v) parameters were estimated using maximum likelihood. Due to the exponential nature
1148 of bacterial growth, and because our data sets contain a number of zeroes, we
1149 transformed our data using the hyperbolic arcsine function ($asinh(x) = ln(x + \sqrt{1 + x^2})$)
1150 [60], which is approximately logarithmic but defined at x=0. The functions lm and logLik
1151 in R were used to calculate log-likelihood under a linear model; optimization was carried
1152 out in R using optim with the Nelder-Mead method. Standard errors of the parameters
1153 were calculated from the Hessian matrix. Fitted values for D and v are given in Table 1
1154 and Table S1. In addition, we generated a phenotype-independent estimate of α using
1155 death rate data from a separate set of time-kill experiments (such as those in Fig. 1) at
1156 formaldehyde concentrations between 3 and 20 mM. Time-kill curves were conducted
1157 as described above, the death rate at each concentration (h^{-1}) was calculated using
1158 linear regression, and the relationship between concentration and death rate was then
1159 also calculated using linear regression. By this method, we estimated α as 0.189±0.010
1160 h^{-1}*mM^{-1}, which fell within the range of values predicted by fitting α for the models we
1161 tested, and within the 95% confidence interval of the estimate of α in the best model.
1162 This phenotype-independent estimate was not used in modeling, but helped to verify
1163 that the values we obtained by parameter fitting were reasonable.

1164

1165 *Model evaluation*

For each experimental condition, we used a likelihood ratio test on the nested models using a forward, stepwise procedure to choose the model that best fit the experimental data. For the formaldehyde selection scenario, the "absolute death" model (with α as the only parameter) was used as the null model, and each 2-parameter model (with alpha and either b, D, or v) was compared against it. Of the three 2-parameter models, we chose the one with the highest likelihood as long as it was significantly better than the null model. If a 2-parameter model was chosen, it became the null model and the procedure was repeated to determine whether a 3-parameter model was supported, and subsequently the 4-parameter model. For the regrowth scenarios, where no death due to formaldehyde is possible, we omitted α and b. We first compared two 1-parameter models (v only or D only) against a null model containing neither, and then evaluated whether adding the second parameter was significantly better. LR was calculated as

$$LR = -2(LL_0 - LL_1)$$

where LL_0 is the log-likelihood of a reduced model and LL_1 is the log-likelihood of the model being tested. Statistical significance was assessed using the chi-squared test, with degrees of freedom given by the difference in the number of parameters between the model being tested and the null model.

1184 **References**

1185

1186 1. Harms A, Fino C, Sørensen MA, Semsey S, Gerdes K. Prophages and growth
1187 dynamics confound experimental results with antibiotic-tolerant persister cells.
1188 mBio. 2017;8: e01964-17. doi:10.1128/mBio.01964-17

1189 2. Shaffer SM, Dunagin MC, Torborg SR, Torre EA, Emert B, Krepler C, et al. Rare
1190 cell variability and drug-induced reprogramming as a mode of cancer drug
1191 resistance. Nature. 2017;546: 431–435. doi:10.1038/nature22794

1192 3. Lorenzi T, Chisholm RH, Desvillettes L, Hughes BD. Dissecting the dynamics of
1193 epigenetic changes in phenotype-structured populations exposed to fluctuating
1194 environments. J Theor Biol. 2015;386: 166–176. doi:10.1016/j.jtbi.2015.08.031

1195 4. Vasdekis AE, Silverman AM, Stephanopoulos G. Origins of cell-to-cell
1196 bioprocessing diversity and implications of the extracellular environment revealed
1197 at the single-cell level. Sci Rep. 2015;5: 17689. doi:10.1038/srep17689

1198 5. Elowitz MB, Levine AJ, Siggia ED, Swain PS. Stochastic gene expression in a
1199 single cell. Science. 2002;297: 1183–1186. doi:10.1126/science.1070919

1200 6. Kiviet DJ, Nghe P, Walker N, Boulineau S, Sunderlikova V, Tans SJ. Stochasticity
1201 of metabolism and growth at the single-cell level. Nature. 2014;514: 376–379.
1202 doi:10.1038/nature13582

1203 7. Newman JRS, Ghaemmaghami S, Ihmels J, Breslow DK, Noble M, DeRisi JL, et
1204 al. Single-cell proteomic analysis of *S. cerevisiae* reveals the architecture of
1205 biological noise. Nature. 2006;441: 840. doi:10.1038/nature04785

1206 8. Bergmiller T, Ackermann M. Pole age affects cell size and the timing of cell division
1207 in *Methylobacterium extorquens* AM1. J Bacteriol. 2011;193: 5216–5221.
1208 doi:10.1128/JB.00329-11

1209 9. Levy SF, Ziv N, Siegal ML. Bet hedging in yeast by heterogeneous, age-correlated
1210 expression of a stress protectant. PLOS Biol. 2012;10: e1001325.
1211 doi:10.1371/journal.pbio.1001325

1212 10. Huh D, Paulsson J. Random partitioning of molecules at cell division. Proc Natl
1213 Acad Sci U S A. 2011;108: 15004–15009. doi:10.1073/pnas.1013171108

1214 11. Ackermann M. A functional perspective on phenotypic heterogeneity in
1215 microorganisms. Nat Rev Microbiol. 2015;13: 497–508. doi:10.1038/nrmicro3491

1216 12. Balaban NQ, Merrin J, Chait R, Kowalik L, Leibler S. Bacterial persistence as a
1217 phenotypic switch. Science. 2004;305: 1622–1625. doi:10.1126/science.1099390

1218 13. Veening J-W, Stewart EJ, Berngruber TW, Taddei F, Kuipers OP, Hamoen LW.
1219 Bet-hedging and epigenetic inheritance in bacterial cell development. Proc Natl
1220 Acad Sci. 2008;105: 4393–4398. doi:10.1073/pnas.0700463105

1221 14. Choi PJ, Cai L, Frieda K, Xie XS. A stochastic single-molecule event triggers
1222 phenotype switching of a bacterial cell. Science. 2008;322: 442.
1223 doi:10.1126/science.1161427

1224 15. Venturelli OS, Zuleta I, Murray RM, El-Samad H. Population diversification in a
1225 yeast metabolic program promotes anticipation of environmental shifts. PLOS Biol.
1226 2015;13: e1002042. doi:10.1371/journal.pbio.1002042

1227 16. Wang J, Atolia E, Hua B, Savir Y, Escalante-Chong R, Springer M. Natural
1228 variation in preparation for nutrient depletion reveals a cost–benefit tradeoff. PLOS
1229 Biol. 2015;13: e1002041. doi:10.1371/journal.pbio.1002041

1230 17. Eldar A, Elowitz MB. Functional roles for noise in genetic circuits. Nature.
1231 2010;467: 167–173. doi:10.1038/nature09326

1232 18. Fridman O, Goldberg A, Ronin I, Shoresh N, Balaban NQ. Optimization of lag time
1233 underlies antibiotic tolerance in evolved bacterial populations. Nature. 2014;513:
1234 418–421. doi:10.1038/nature13469

1235 19. Rainey PB, Beaumont HJ, Ferguson GC, Gallie J, Kost C, Libby E, et al. The
1236 evolutionary emergence of stochastic phenotype switching in bacteria. Microb Cell
1237 Factories. 2011;10: S14. doi:10.1186/1475-2859-10-S1-S14

1238 20. Chisholm RH, Lorenzi T, Desvillettes L, Hughes BD. Evolutionary dynamics of
1239 phenotype-structured populations: from individual-level mechanisms to population-
1240 level consequences. Z Für Angew Math Phys. 2016;67: 100. doi:10.1007/s00033-
1241 016-0690-7

1242 21. Klironomos FD, Berg J, Collins S. How epigenetic mutations can affect genetic
1243 evolution: Model and mechanism. BioEssays. 2013;35: 571–578.
1244 doi:10.1002/bies.201200169

1245 22. Levin-Reisman I, Ronin I, Gefen O, Braniss I, Shoresh N, Balaban NQ. Antibiotic
1246 tolerance facilitates the evolution of resistance. Science. 2017;355: 826–830.
1247 doi:10.1126/science.aaj2191

1248 23. Deris JB, Kim M, Zhang Z, Okano H, Hermsen R, Groisman A, et al. The innate
1249 growth bistability and fitness landscapes of antibiotic-resistant bacteria. Science.
1250 2013;342: 1237435. doi:10.1126/science.1237435

1251 24. Lorenzi T, Chisholm RH, Clairambault J. Tracking the evolution of cancer cell
1252 populations through the mathematical lens of phenotype-structured equations. Biol
1253 Direct. 2016;11: 43. doi:10.1186/s13062-016-0143-4

1254 25. Fall R, Benson AA. Leaf methanol — the simplest natural product from plants.
1255 Trends Plant Sci. 1996;1: 296–301. doi:10.1016/S1360-1385(96)88175-0

1256 26. Skovran E, Crowther GJ, Guo X, Yang S, Lidstrom ME. A systems biology
1257 approach uncovers cellular strategies used by *Methylobacterium extorquens* AM1
1258 during the switch from multi- to single-carbon growth. PLoS ONE. 2010;5: e14091.
1259 doi:10.1371/journal.pone.0014091

1260 27. Nayak DD, Marx CJ. Genetic and phenotypic comparison of facultative
1261 methylotrophy between *Methylobacterium extorquens* strains PA1 and AM1. PLoS
1262 ONE. 2014;9: e107887. doi:10.1371/journal.pone.0107887

1263 28. Chen NH, Djoko KY, Veyrier FJ, McEwan AG. Formaldehyde stress responses in
1264 bacterial pathogens. Front Microbiol. 2016;7. doi:10.3389/fmicb.2016.00257

1265 29. Marx CJ, Chistoserdova L, Lidstrom ME. Formaldehyde-detoxifying role of the
1266 tetrahydromethanopterin-linked pathway in *Methylobacterium extorquens* AM1. J
1267 Bacteriol. 2003;185: 7160–7168. doi:10.1128/JB.185.23.7160-7168.2003

1268 30. Atwood KC, Norman A. On the interpretation of multi-hit survival curves. Proc Natl
1269 Acad Sci U S A. 1949;35: 696–709.

1270 31. Peleg M. Microbial survival curves — the reality of flat “shoulders” and absolute
1271 thermal death times. Food Res Int. 2000;33: 531–538. doi:10.1016/S0963-
1272 9969(00)00088-0

1273 32. Regoes RR, Wiuff C, Zappala RM, Garner KN, Baquero F, Levin BR.
1274 Pharmacodynamic functions: a multiparameter approach to the design of antibiotic
1275 treatment regimens. Antimicrob Agents Chemother. 2004;48: 3670–3676.
1276 doi:10.1128/AAC.48.10.3670-3676.2004

1277 33. Levin BR, Udekwu KI. Population dynamics of antibiotic treatment: a mathematical
1278 model and hypotheses for time-kill and continuous-culture experiments. Antimicrob
1279 Agents Chemother. 2010;54: 3414–3426. doi:10.1128/AAC.00381-10

1280 34. Yurtsev EA, Chao HX, Datta MS, Artemova T, Gore J. Bacterial cheating drives the
1281 population dynamics of cooperative antibiotic resistance plasmids. Mol Syst Biol.
1282 2013;9: 683. doi:10.1038/msb.2013.39

1283 35. Lennon JT, Jones SE. Microbial seed banks: the ecological and evolutionary
1284 implications of dormancy. Nat Rev Microbiol. 2011;9: 119–130.
1285 doi:10.1038/nrmicro2504

1286 36. Kotte O, Volkmer B, Radzikowski JL, Heinemann M. Phenotypic bistability in
1287 *Escherichia coli*'s central carbon metabolism. Mol Syst Biol. 2014;10: 736–736.
1288 doi:10.15252/msb.20135022

1289 37. Boxtel C van, Heerden JH van, Nordholt N, Schmidt P, Bruggeman FJ. Taking
1290 chances and making mistakes: non-genetic phenotypic heterogeneity and its
1291 consequences for surviving in dynamic environments. J R Soc Interface. 2017;14:
1292 20170141. doi:10.1098/rsif.2017.0141

1293 38. Levin-Reisman I, Fridman O, Balaban NQ. ScanLag: High-throughput
1294 quantification of colony growth and lag time. J Vis Exp JoVE. 2014;
1295 doi:10.3791/51456

1296 39. Guillier L, Pardon P, Augustin J-C. Automated image analysis of bacterial colony
1297 growth as a tool to study individual lag time distributions of immobilized cells. J
1298 Microbiol Methods. 2006;65: 324–334. doi:10.1016/j.mimet.2005.08.007

1299 40. Ernebjerg M, Kishony R. Distinct growth strategies of soil bacteria as revealed by
1300 large-scale colony tracking. Appl Environ Microbiol. 2012;78: 1345–1352.
1301 doi:10.1128/AEM.06585-11

1302 41. Mitsui R, Kusano Y, Yurimoto H, Sakai Y, Kato N, Tanaka M. Formaldehyde
1303 fixation contributes to detoxification for growth of a nonmethylotroph, *Burkholderia*
1304 *cepacia* TM1, on vanillic acid. Appl Environ Microbiol. 2003;69: 6128–6132.
1305 doi:10.1128/AEM.69.10.6128-6132.2003

1306 42. Sudtachat N, Ito N, Itakura M, Masuda S, Eda S, Mitsui H, et al. Aerobic vanillate
1307 degradation and C1 compound metabolism in *Bradyrhizobium japonicum*. Appl
1308 Environ Microbiol. 2009;75: 5012–5017. doi:10.1128/AEM.00755-09

1309 43. Peredo EL, Simmons SL. Leaf-FISH: microscale imaging of bacterial taxa on
1310 phyllosphere. Front Microbiol. 2018;8. doi:10.3389/fmicb.2017.02669

1311 44. Voordeckers K, Kominek J, Das A, Espinosa-Cantú A, Maeyer DD, Arslan A, et al.
1312 Adaptation to high ethanol reveals complex evolutionary pathways. PLOS Genet.
1313 2015;11: e1005635. doi:10.1371/journal.pgen.1005635

1314 45. Costa E, Pérez J, Kreft J-U. Why is metabolic labour divided in nitrification? Trends
1315 Microbiol. 2006;14: 213–219. doi:10.1016/j.tim.2006.03.006

1316 46. Strovas TJ, Sauter LM, Guo X, Lidstrom ME. Cell-to-Cell heterogeneity in growth
1317 rate and gene expression in *Methylobacterium extorquens* AM1. J Bacteriol.
1318 2007;189: 7127–7133. doi:10.1128/JB.00746-07

1319 47. Strovas TJ, Lidstrom ME. Population *in Methylobacterium extorquens* AM1.
1320 Microbiology. 2009;155: 2040–2048. doi:10.1099/mic.0.025890-0

1321 48. Gallie J, Libby E, Bertels F, Remigi P, Jendresen CB, Ferguson GC, et al.
1322 Bistability in a metabolic network underpins the de novo evolution of colony
1323 switching in *Pseudomonas fluorescens*. PLOS Biol. 2015;13: e1002109.
1324 doi:10.1371/journal.pbio.1002109

1325 49. Ozbudak EM, Thattai M, Lim HN, Shraiman BI, van Oudenaarden A. Multistability
1326 in the lactose utilization network of *Escherichia coli*. Nature. 2004;427: 737–740.
1327 doi:10.1038/nature02298

1328 50. Roff DA. The evolution of threshold traits in animals. Q Rev Biol. 1996;71: 3–35.
1329 doi:10.1086/419266

1330 51. Govers SK, Mortier J, Adam A, Aertsen A. Protein aggregates encode epigenetic
1331 memory of stressful encounters in individual *Escherichia coli* cells. PLOS Biol.
1332 2018;16: e2003853. doi:10.1371/journal.pbio.2003853

1333 52. Bandyopadhyay A, Wang H, Ray JCJ. Lineage space and the propensity of
1334 bacterial cells to undergo growth transitions. PLOS Comput Biol. 2018;14:
1335 e1006380. doi:10.1371/journal.pcbi.1006380

1336 53. Kussell E, Leibler S. Phenotypic diversity, population growth, and information in
1337 fluctuating environments. Science. 2005;309: 2075–2078.
1338 doi:10.1126/science.1114383

1339 54. Arnoldini M, Mostowy R, Bonhoeffer S, Ackermann M. Evolution of stress response
1340 in the face of unreliable environmental signals. PLOS Comput Biol. 2012;8:
1341 e1002627. doi:10.1371/journal.pcbi.1002627

1342 55. Beaumont HJE, Gallie J, Kost C, Ferguson GC, Rainey PB. Experimental evolution
1343 of bet hedging. Nature. 2009;462: 90. doi:10.1038/nature08504

1344 56. Draghi J. Links between evolutionary processes and phenotypic robustness in
1345 microbes. Semin Cell Dev Biol. 2018; doi:10.1016/j.semcdb.2018.05.017

1346 57. Abanda-Nkpwatt D, Müsch M, Tschiersch J, Boettner M, Schwab W. Molecular
1347 interaction between *Methylobacterium extorquens* and seedlings: growth
1348 promotion, methanol consumption, and localization of the methanol emission site. J
1349 Exp Bot. 2006;57: 4025–4032. doi:10.1093/jxb/erl173

1350 58. Ryffel F, Helfrich EJN, Kiefer P, Peyriga L, Portais J-C, Piel J, et al. Metabolic
1351 footprint of epiphytic bacteria on *Arabidopsis thaliana* leaves. ISME J. 2016;10:
1352 632–643. doi:10.1038/ismej.2015.141

1353 59. Nemecek-Marshall M, MacDonald RC, Franzen JJ, Wojciechowski CL, Fall R.
1354 Methanol emission from leaves (Enzymatic detection of gas-phase methanol and
1355 relation of methanol fluxes to stomatal conductance and leaf development). Plant
1356 Physiol. 1995;108: 1359–1368. doi:10.1104/pp.108.4.1359

1357 60. Ackermann M. Microbial individuality in the natural environment. ISME J. 2013;7:
1358 465–467. doi:10.1038/ismej.2012.131

1359 61. Delaney NF, Kaczmarek ME, Ward LM, Swanson PK, Lee M-C, Marx CJ.
1360 Development of an optimized medium, strain and high-throughput culturing
1361 methods for *Methylobacterium extorquens*. PLOS ONE. 2013;8: e62957.
1362 doi:10.1371/journal.pone.0062957

1363 62. Nash T. The colorimetric estimation of formaldehyde by means of the Hantzsch
1364 reaction. Biochem J. 1953;55: 416–421.

1365 63. Deatherage DE, Barrick JE. Identification of mutations in laboratory-evolved
1366 microbes from next-generation sequencing data using *breseq*. Engineering and
1367 Analyzing Multicellular Systems. Humana Press, New York, NY; 2014. pp. 165–
1368 188. doi:10.1007/978-1-4939-0554-6_12

1369 64. Marx CJ, Bringel F, Chistoserdova L, Moulin L, Farhan Ul Haque M, Fleischman
1370 DE, et al. Complete genome sequences of six strains of the genus
1371 *Methylobacterium*. J Bacteriol. 2012;194: 4746–4748. doi:10.1128/JB.01009-12

1372 65. Michener JK, Vuilleumier S, Bringel F, Marx CJ. Transfer of a catabolic pathway for
1373 chloromethane in *Methylobacterium* strains highlights different limitations for
1374 growth with chloromethane or with dichloromethane. Front Microbiol. 2016;7.
1375 doi:10.3389/fmicb.2016.01116

1376 66. R Core Team. R: A language and environment for statistical computing. [Internet].
1377 Vienna, Austria: R Foundation for Statistical Computing; 2018. Available:
1378 http://www.R-project.org

1379 67. Hahne F, LeMeur N, Brinkman RR, Ellis B, Haaland P, Sarkar D, et al. flowCore: a
1380 Bioconductor package for high throughput flow cytometry. BMC Bioinformatics.
1381 2009;10: 106. doi:10.1186/1471-2105-10-106

1382 68. Wickham, H. ggplot2: Elegant graphics for data analysis [Internet]. New York:
1383 Springer-Verlag; 2016. Available: http://ggplot2.org

1384 69. van der Walt S, Schönberger JL, Nunez-Iglesias J, Boulogne F, Warner JD, Yager
1385 N, et al. scikit-image: image processing in Python. PeerJ. 2014;2: e453.
1386 doi:10.7717/peerj.453

1387 70. Schneider CA, Rasband WS, Eliceiri KW. NIH Image to ImageJ: 25 years of image
1388 analysis. Nat Methods. 2012;9: 671–675.

71. Wilcoxon F. Individual comparisons by ranking methods. Biom Bull. 1945;1: 80–83. doi:10.2307/3001968

72. Anderson MJ. A new method for non-parametric multivariate analysis of variance. Austral Ecol. 2001;26: 32–46. doi:10.1111/j.1442-9993.2001.01070.pp.x

73. Oksanen J, Blanchet FG, Kindt R, Legendre P, Minchin PR, O'Hara RB, et al. The vegan package. Community Ecol Package. 2007;10: 631–637.

74. McAllister CF, Lepo JE. Succinate transport by free-living forms of *Rhizobium japonicum*. J Bacteriol. 1983;153: 1155–1162.

75. Anthony C, Zatman LJ. The microbial oxidation of methanol. 2. The methanol-oxidizing enzyme of *Pseudomonas* sp. M27. Biochem J. 1964;92: 614–621.

76. Soetaert K, Meysman F. Reactive transport in aquatic ecosystems: Rapid model prototyping in the open source software R. Environ Model Softw. 2012;32: 49–60. doi:10.1016/j.envsoft.2011.08.011

77. Stoetaert K, Petzoldt T, Setzer W. Solving differential equations in R: package deSolve. J Stat Softw. 2010;33: 1–25. doi:10.18637/jss.v033.i09

78. Hindmarsh AC. ODEPACK, A systematized collection of ODE solvers. In: Stepleman RS, editor. Scientific Computing. Amsterdam: North-Holland; 1983. pp. 55–64.

1409 **Figures with legends**

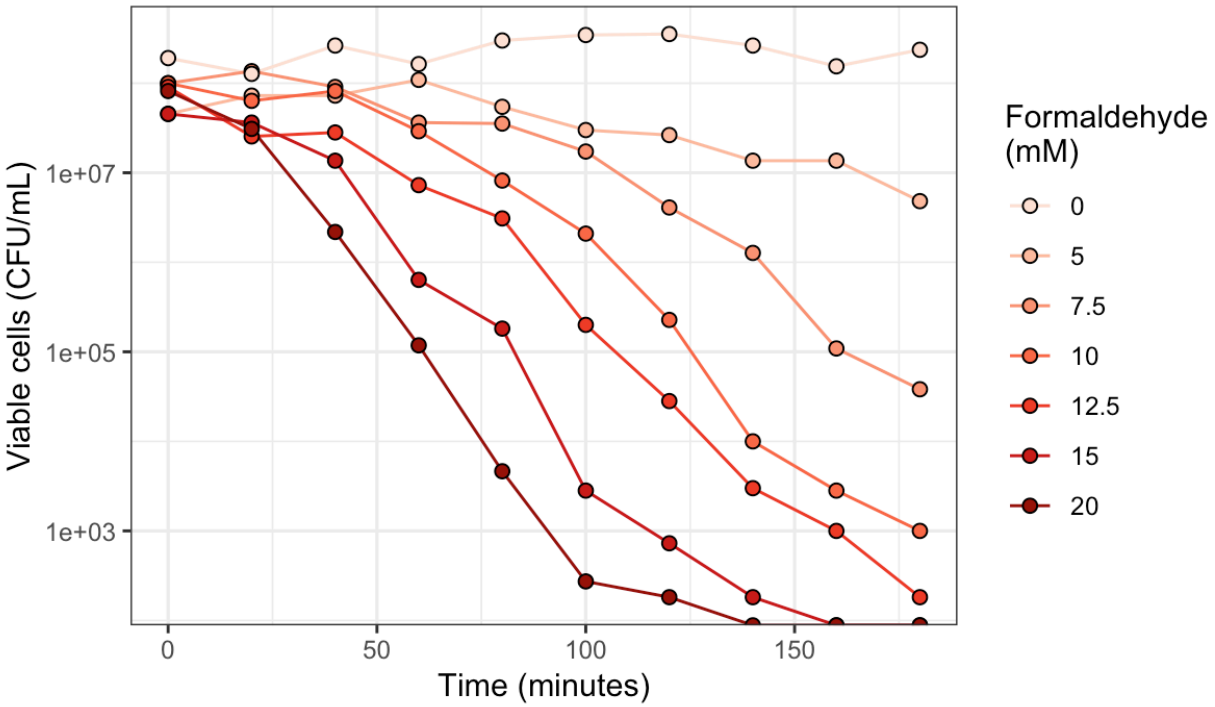

1410
1411 **Figure 1. Formaldehyde kills *M. extorquens* at an exponential, concentration-**
1412 **dependent rate.**
1413 Formaldehyde was added at the indicated concentrations to liquid cultures of *M.*
1414 *extorquens* cells growing in minimal medium with methanol, and abundance of viable
1415 cells was measured as colony-forming units (CFU) over time. Note that negligible
1416 growth is expected to have occurred during the course of this experiment, as the 180-
1417 minute duration was less than one generation (~3.5 hrs) for *M. extorquens* in these
1418 conditions.

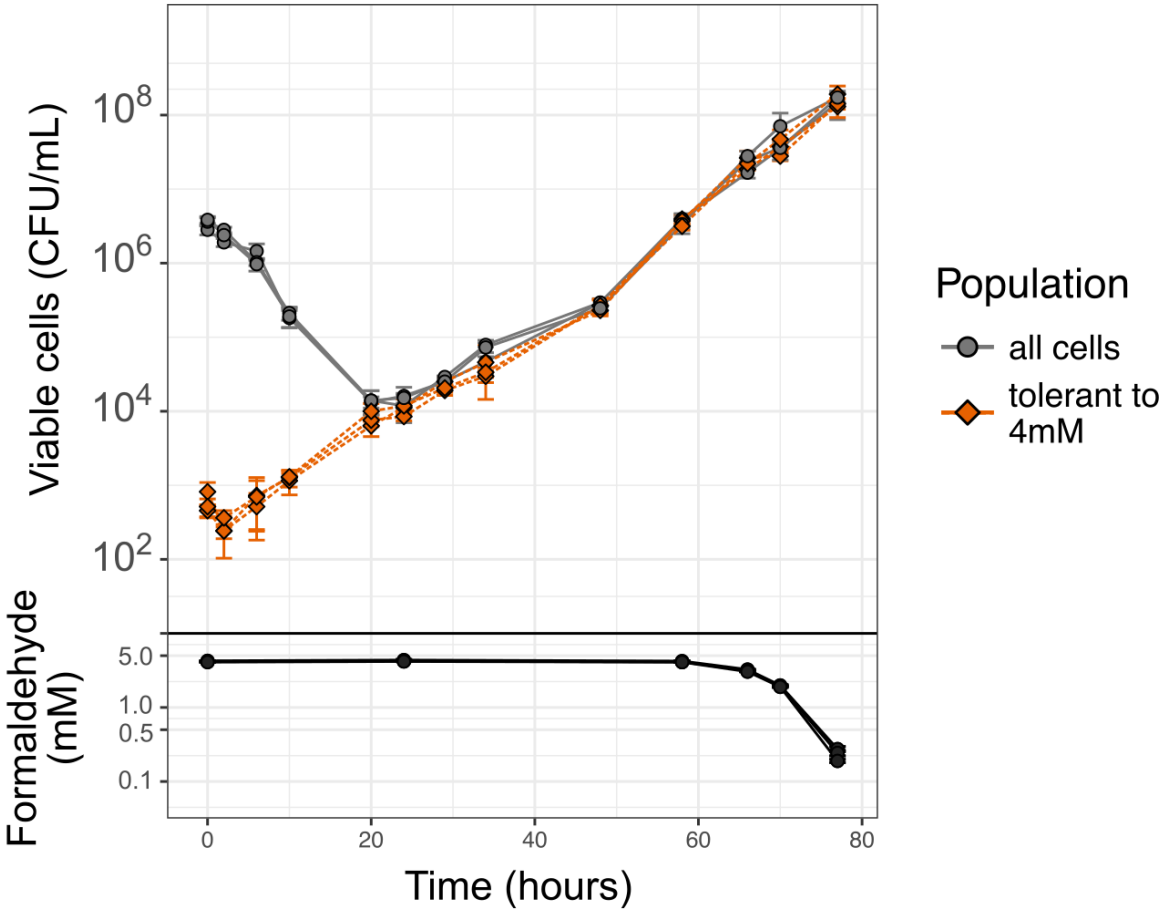

1419
1420 **Figure 2. Re-growth of *M. extorquens* after population decline in the presence of**
1421 **formaldehyde is due to a pre-existing sub-population of formaldehyde-tolerant**
1422 **cells.**
1423 Stationary-phase cells were inoculated into fresh medium containing methanol and 4
1424 mM formaldehyde. The abundance of viable cells in the two different populations was
1425 assessed over time by removing and washing cells, then plating onto both permissive
1426 medium (without formaldehyde: "all cells") and selective medium (with 4 mM
1427 formaldehyde: "tolerant to 4 mM"). CFU = colony-forming units. Each line represents
1428 one biological replicate; error bars show the standard deviation of three replicate
1429 platings. Formaldehyde in the liquid medium during the incubation period was measured
1430 by a colorimetric assay on subsamples after removing cells by centrifugation.

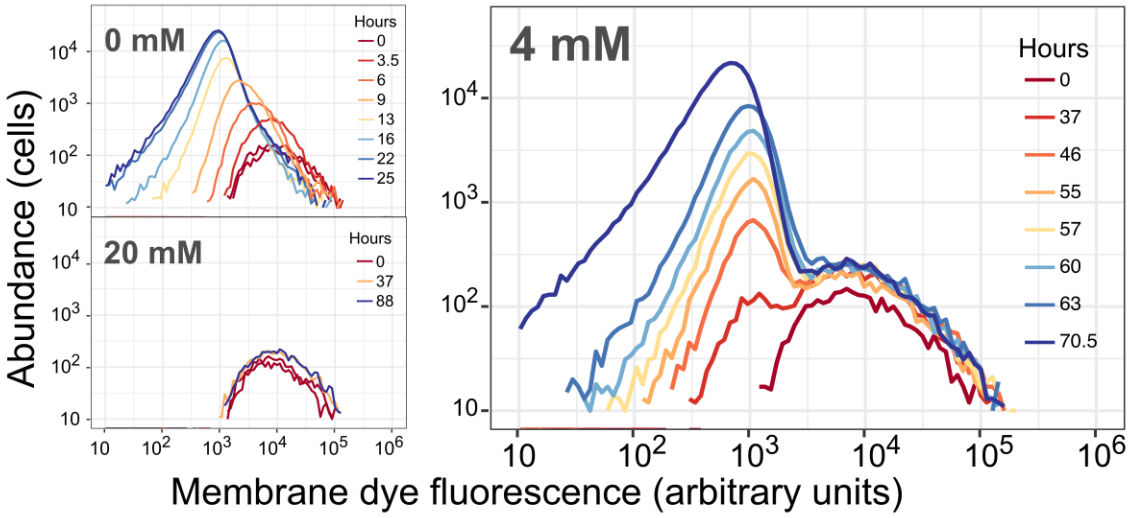

Figure 3. **Cell proliferation assay shows dynamics consistent with the coexistence of both growing and non-growing subpopulations, with no turnover between the two**.
Cells were stained with PKH67 fluorescent membrane dye, then allowed to grow in minimal medium with methanol and either 0, 4, or 20 mM formaldehyde. Histograms show per-cell fluorescence of the cells (events measured by flow cytometry) present in 30 µL of culture at each timepoint; colors denote the time of sampling in hours (note that different color scales are used in different panels). Top left: without formaldehyde, all cells underwent doubling, diluting their membrane fluorescence so that the median fluorescence decreased as population increased. Bottom left: at high concentrations of formaldehyde, no cells grew, leaving per-cell fluorescence unchanged. Right: in the presence of 4 mM formaldehyde, most cells did not grow, but a few did; consequently, a small growing population with lower per-cell fluorescence became detectable at 37 hours and continued to increase in abundance thereafter. Results of experiments conducted at other formaldehyde concentrations are shown in Fig. S5.

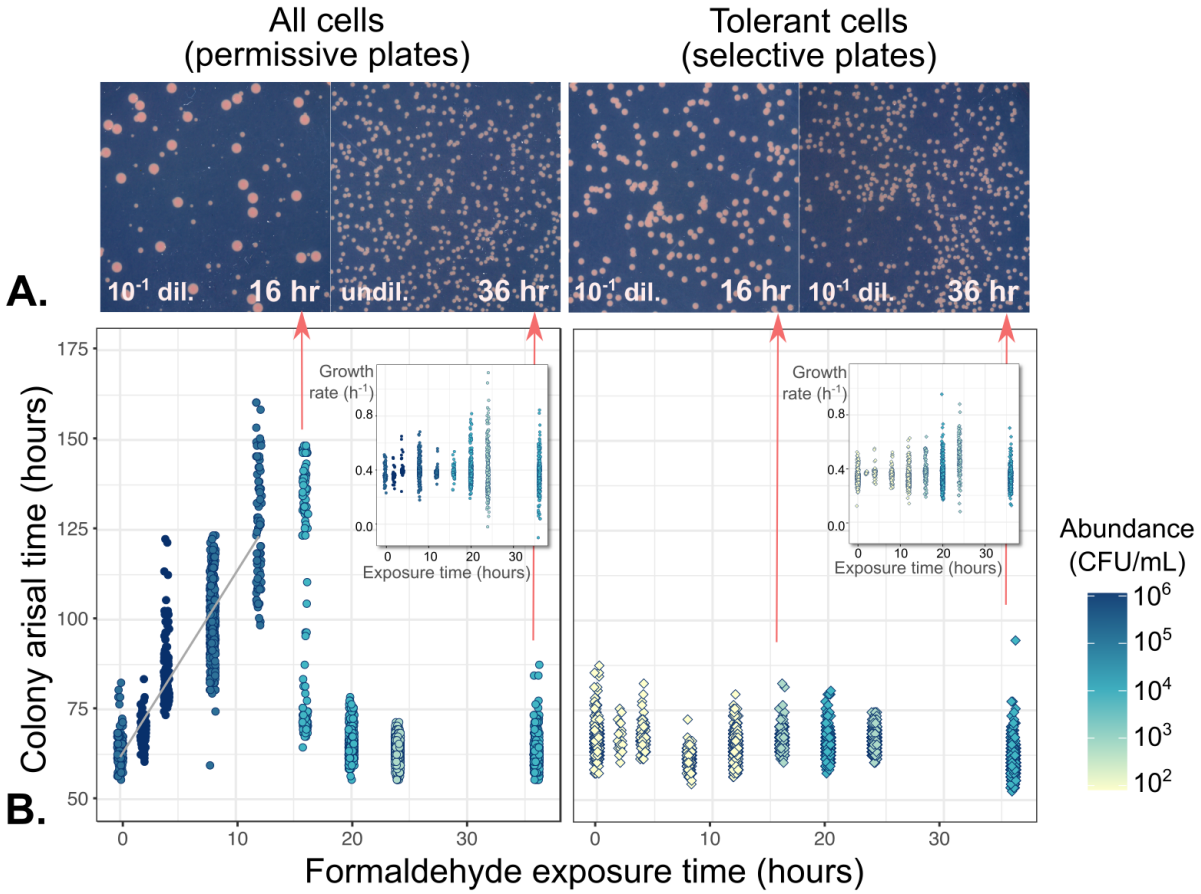

Figure 4. **Cell damage by formaldehyde results in delayed colony arisal for the majority of cells, but not for the tolerant subpopulation.**
Cells from a formaldehyde exposure experiment (liquid MPIPES medium with 4 mM formaldehyde) were sampled at 2- to 4-hour intervals, washed, and plated onto both permissive medium (no formaldehyde, allowing the growth of all cells) and selective medium (4 mM formaldehyde, allowing the growth of only the tolerant subpopulation). A) Images of colonies on plates. Colony size heterogeneity was evident only on permissive medium with cultures exposed to formaldehyde for 16 hours, consistent with a population containing both sensitive cells that formed colonies late due to formaldehyde-induced damage (small colonies) and tolerant cells that formed colonies early (large colonies). All images are shown at the same magnification level; *dil*=dilution factor prior to plating. B) Relationship between formaldehyde exposure and colony growth characteristics. Shading indicates abundance of colony-forming units in each population (see Fig. 2); samples were diluted prior to plating for an average of 500 colonies per plate. Left panel: gray line shows linear regression of arisal time on exposure time for the first 12 hours. Every hour of exposure to formaldehyde led to a ~4.8-hour delay in colony arisal time among sensitive cells. At 16 hours, the population consisted of both damaged and tolerant cells; after 20 hours, all cells were tolerant due to the death of the damaged cells. Right panel: among tolerant cells, formaldehyde exposure had no effect on arisal time. Insets: exposure time affected only the variability among colony growth rates, but not their median.

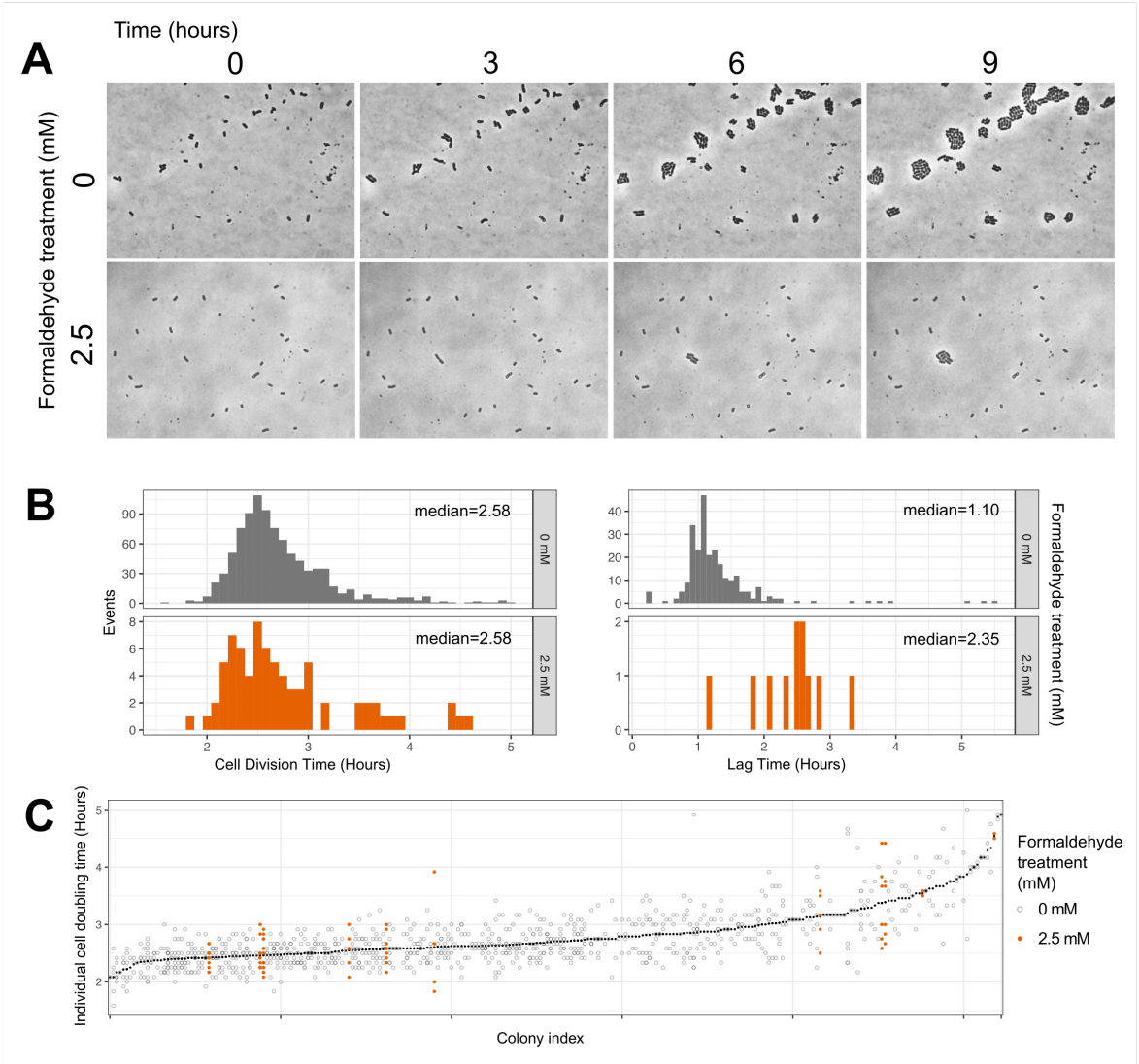

Figure 5. Time-lapse microscopy reveals binary (i.e., growth or non-growth) phenotypes in response to formaldehyde.
A) Example images: cells were embedded in agar medium with methanol and either 0 mM (top) or 2.5 mM (bottom) formaldehyde and monitored for 9 hours (~3 generations). At 0 mM, 256 cells were observed and all underwent at least one doubling; at 2.5 mM, 546 cells were observed and 11 (1.97%) underwent at least one doubling, in accordance with our predictions for this formaldehyde concentration (see Fig. 6). B) Histograms of cell division time (across all generations) and lag time (time between deposition and first cell division, for each microcolony) for cells that grew. No difference was observed in cell division time between the two treatments (p=0.262, Mann-Whitney Wilcoxon test). However, cells in formaldehyde took approximately 1.25 hours longer to reach the first cell division (p<0.001, Mann-Whitney). C) Scatterplot of individual cell doubling times; each position along the x-axis represents a single microcolony, ordered by mean doubling time (shown in black symbols). Individual doubling time of each cell was strongly predicted by the colony it came from (p=0.001) but not by formaldehyde treatment (p=0.323, PERMANOVA).

1486

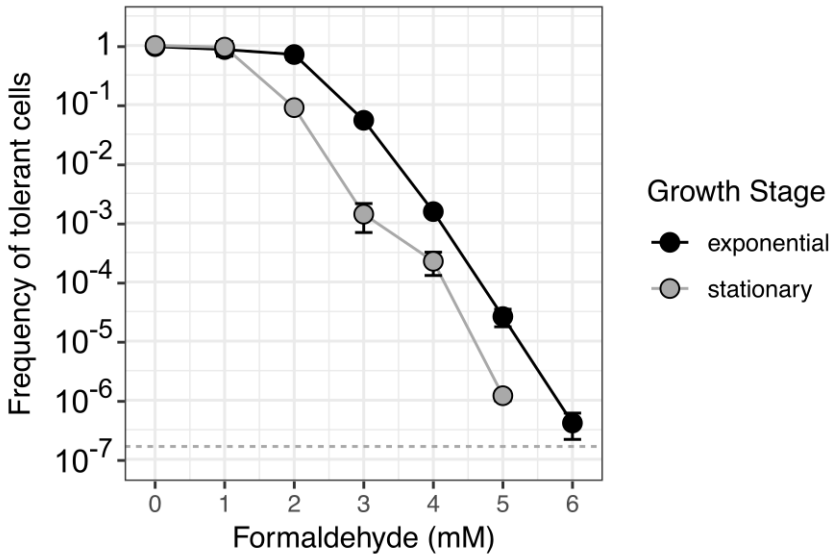

1487

1488 **Figure 6**. **Subpopulations of formaldehyde-tolerant cells are distributed within a**
1489 **wild-type population with continuous, exponentially-decreasing frequency.**
1490 *M. extorquens* cells not previously exposed to formaldehyde were plated onto methanol
1491 agar medium containing a range of formaldehyde concentrations at 1-mM intervals. The
1492 frequency of tolerant cells is expressed as the ratio of the colony-forming units (CFU) on
1493 formaldehyde medium at the specified concentration to the CFU on formaldehyde-free
1494 (0 mM) medium. Error bars denote the standard deviation of replicate experiments from
1495 5 different dates (shown individually in Fig. S4). Detection limit is indicated by the
1496 dashed horizontal line.

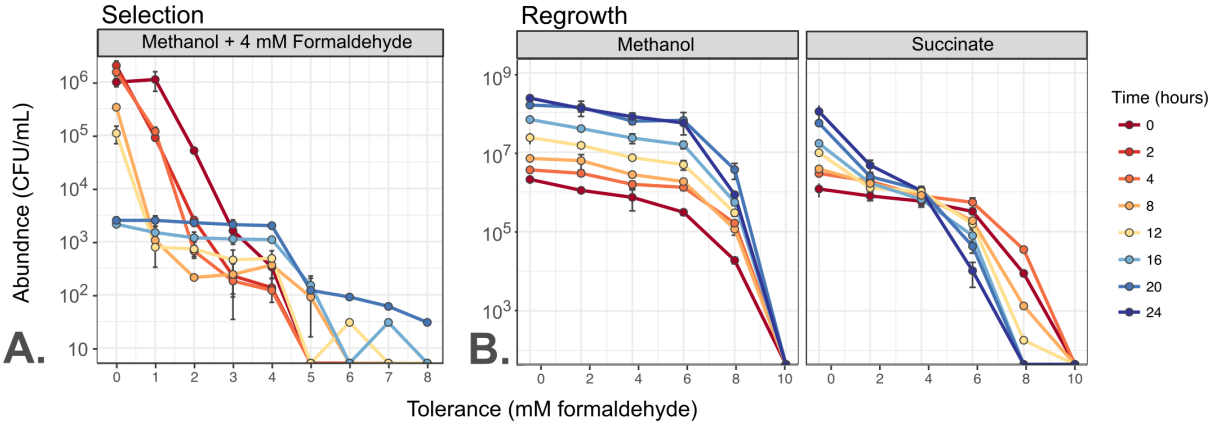

1497
1498 **Figure 7. The distribution of formaldehyde tolerance within an *M. extorquens***
1499 **population changes over time depending on growth conditions.**
1500 Plots show total abundance (not frequency) of cells tolerant to each level of
1501 formaldehyde, as assessed by plating onto selective medium; each colored line
1502 represents one timepoint and error bars represent the standard deviation of three
1503 plating replicates. For clarity, only one biological replicate is shown; results from other
1504 replicates are shown in Fig. S6. Populations were tested for tolerance at up to 10 mM
1505 (panel A) or 12 mM (panel B), but 0 CFU were detected above the tolerance levels
1506 shown here. A) Exposure of a naive population to 4 mM formaldehyde results in rapid
1507 decline of subpopulations with tolerance levels <4 mM and selective growth of
1508 subpopulations with tolerance levels ≥4 mM. B) When the population from A), enriched
1509 in tolerant cells, is transferred to medium without formaldehyde, tolerance distribution
1510 dynamics depend on the growth substrate provided. If growth occurs on methanol, all
1511 subpopulations grow equally well: the enrichment of formaldehyde-tolerant populations
1512 is retained for the full 24 hours (~7 generations) of observation. If growth occurs on
1513 succinate, subpopulations with high tolerance decline in abundance and those with low
1514 tolerance increase: the population reverts to its original naive distribution.

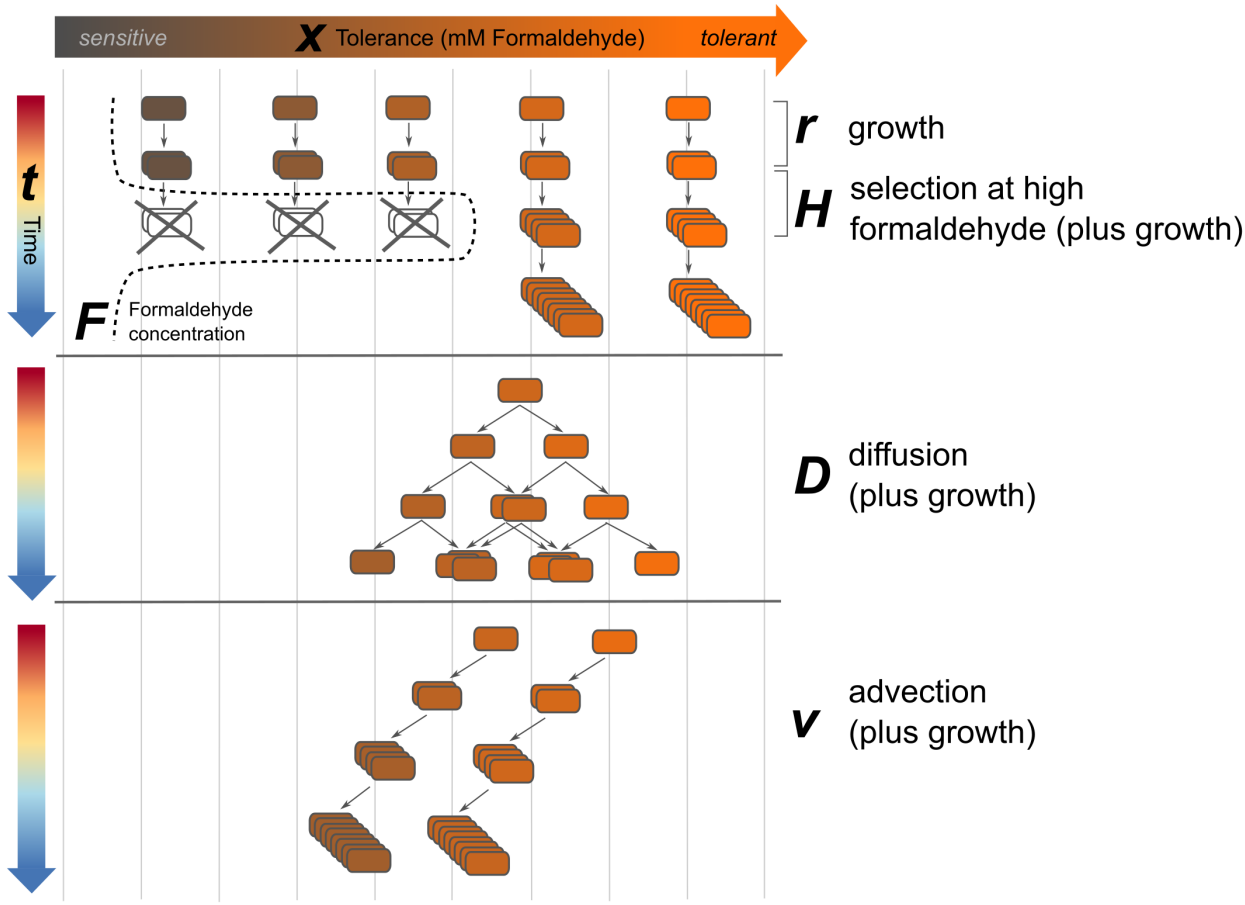

Figure 8. Schematic of processes described by mathematical model of tolerance distribution dynamics.
Cells exist in 1-dimensional phenotype space along a continuum from sensitive to tolerant, with *x* denoting the maximum concentration of formaldehyde (*F*) at which a cell can grow. Under normal growth (at rate *r*), progeny cells carry the same tolerance phenotype as their parents. Exposure to formaldehyde results in the death of low-tolerance ($x<F$) phenotypes at a rate described by $H(x, F)$. In the process of diffusion, cells and their progeny shift to adjacent tolerant states according to the diffusion constant *D*, resulting in the broadening of the population's tolerance distribution. In advection, cells and their progeny move in a single direction in tolerance space at rate *v*, resulting in an overall shift in the population's distribution toward either lower or higher average tolerance.

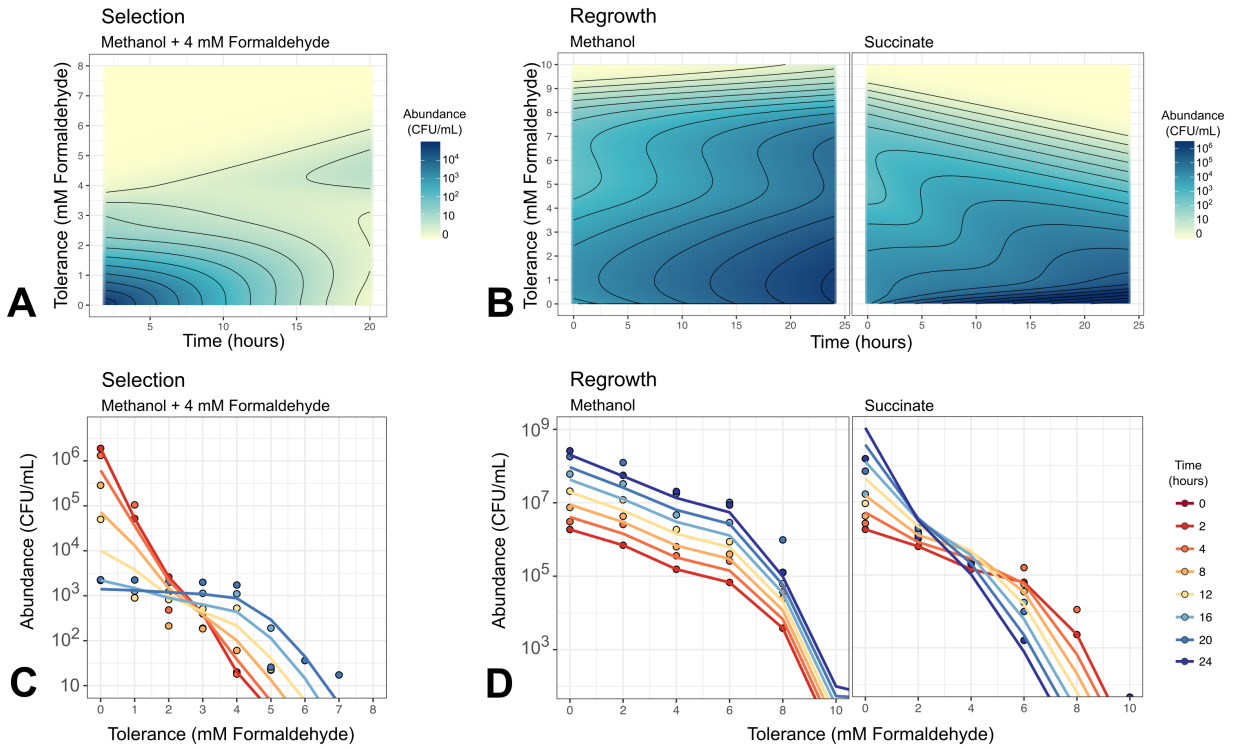

Figure 9. Mathematical modeling reproduces growth, death, and phenotype transition dynamics of *M. extorquens* population under multiple conditions. A) and B) Heat maps showing model simulations of population dynamics. Model parameters as given in Table 1. Note that model results are continuous in phenotype space, and non-cumulative (the abundance at concentration *x* shows only the number of cells for which that is the maximum concentration tolerable, not the number of all cells that can grow at that concentration; see Methods for details). C) and D) Comparison of model results (lines) and experimental data (points). Experimental data are averages of 3 biological replicates; model results have been binned at 1- or 2-mM intervals, and summed to form cumulative distributions, to facilitate comparison. A and C) 4 mM formaldehyde exposure experiment, resulting in selection of cells with >4 mM tolerance. B and D) Formaldehyde-free regrowth experiment, in which the selected high-tolerance population is transferred to medium without formaldehyde and either methanol or succinate as the carbon substrate, resulting in different shifts in phenotype distribution.

Table 1. Comparison of possible models describing formaldehyde-tolerance phenotype transition processes of *M. extorquens* populations.

For each combination of culture condition and growth substrate, we used a stepwise procedure to evaluate nested models using a likelihood ratio test. Shown below are the best-fit values for the four fitted parameters in each of those models, and test results for each model. *α*: dependence of death rate on formaldehyde ($h^{-1}*mM^{-1}$). *v*: advection rate ($mM*h^{-1}$). *D*: diffusion constant (mM^2*h^{-1}). (for *v* and *D*, mM denotes tolerance). *b*: dependence of death rate on individual tolerance level (mM tolerance / mM formaldehyde in medium). For the likelihood ratio test, name of the model used as the null model, as well as the χ^2 value and *p*-value, are given. Gray shading: the best-supported model for that experimental scenario. Pseudo-R^2 values for those models were: for formaldehyde selection, 0.973; for methanol regrowth, 0.993; for succinate regrowth, 0.991.

Model	***Experimental scenario***		***Parameters***				***Likelihood Ratio Test***		
	Condition	**Substrate**	***α***	***b***	***v***	***D***	**null model**	χ^2	***p***
F1	selection	Methanol + Formaldehyde	0.152	n/a	n/a	n/a	n/a	n/a	n/a
F2a	selection	Methanol + Formaldehyde	0.177	0.800	n/a	n/a	F1	0.914	0.339
F2b	selection	Methanol + Formaldehyde	0.156	n/a	-0.020	n/a	F1	17.455	3E-05
F2c	selection	Methanol + Formaldehyde	0.160	n/a	n/a	0.026	F1	18.480	2E-05
F3a	selection	Methanol + Formaldehyde	0.202±0.022	0.770±0.147	n/a	0.019±0.006	F2b	9.379	0.002
F3b	selection	Methanol + Formaldehyde	0.165	n/a	-0.034	0.007	F2b	1.647	0.199
F4	selection	Methanol + Formaldehyde	0.204	0.791	0.007	0.022	F3a	0.029	0.865
M0	regrowth	Methanol	n/a	n/a	n/a	n/a	n/a	n/a	n/a
M1a	regrowth	Methanol	n/a	n/a	0.018±0.006	n/a	M0	7.843	0.005
M1b	regrowth	Methanol	n/a	n/a	n/a	4.94×10^{9}	M0	0.000	1.000
M2	regrowth	Methanol	n/a	n/a	1.85×10^{-2}	4.60×10^{-8}	M1a	-0.008	1.000
S0	regrowth	Succinate	n/a	n/a	n/a	n/a	n/a	n/a	n/a
S1a	regrowth	Succinate	n/a	n/a	0.189	n/a	S0	97.197	<0.001
S1b	regrowth	Succinate	n/a	n/a	n/a	6.43×10^{9}	S0	0.000	1.000
S2	regrowth	Succinate	n/a	n/a	0.285±0.026	0.033±0.010	S1a	15.918	<0.001

1558 **Supporting Information**
1559
1560 Figure S1. Formaldehyde concentrations of ≤5 mM allow growth of *M. extorquens* at a
1561 normal rate, but only after a period of lag; higher concentrations lead to longer lag
1562 times.
1563
1564 Figure S2. Image processing pipeline to generate colony growth data from
1565 formaldehyde-exposed cultures.
1566
1567 Figure S3. Formaldehyde tolerance may be associated with lower fitness on a
1568 multicarbon substrate.
1569
1570 Figure S4. Formaldehyde tolerance distributions in *Methylobacterium* populations are
1571 robust across experimental replicates, but vary depending on growth conditions.
1572
1573 Figure S5. Cell proliferation assays support the hypothesis that growth of *M. extorquens*
1574 in the presence of formaldehyde is due to a small subpopulation of tolerant cells, and
1575 that the abundance of tolerant cells decreases with increasing formaldehyde.
1576
1577 Figure S6. The distribution of formaldehyde tolerance within an *M. extorquens*
1578 population changes over time depending on growth conditions.
1579
1580 Figure S7. Estimation of growth rates and initial conditions for use in the mathematical
1581 model.
1582
1583 Figure S8. The parameter *b* (dependence of death rate on formaldehyde tolerance)
1584 determines the shape of the population's phenotypic tolerance distribution after
1585 exposure to formaldehyde.
1586
1587 Figure S9. Formaldehyde concentrations in agar growth medium are stable over time
1588 and reflective of similar concentrations in liquid medium.
1589
1590 Figure S10. Time-lapse microscopy: cell segmentation and tracking.
1591
1592 Figure S11. Models using extended and original tolerance distributions perform
1593 similarly.
1594
1595 Table S1. Results of model selection using original data set for fitting (distribution not
1596 extended to account for experimental limit of detection).
1597
1598 File S1. Modeling phenotypic switching in *Methylobacterium extorquens*: R notebook
1599